COMPLEMENT COMPONENT C5 AND GRAFT-VERSUS-HOST-DISEASE

GENE EDITING OF COMPLEMENT COMPONENT C5 TO PREVENT GRAFT-VERSUS-HOST-DISEASE FOLLOWING ALLOGENEIC-HEMATOPOIETIC STEM CELL TRANSPLANT

By EKATERINA TODOROVA, H.B.Sc

A Thesis Submitted to the School of Graduate Studies in Partial Fulfillment of the Requirements

for the Degree Master of Science

McMaster University MASTER OF SCIENCE (2019) Hamilton, Ontario

TITLE: Gene Editing of Complement Component C5 to Prevent Graft-Versus-Host-Disease Following Allogeneic-Hematopoietic Stem Cell Transplant

AUTHOR: Ekaterina Todorova, H.B.Sc (University of Western Ontario, London Ontario)

SUPERVISOR: Dr. Mark Larché

PAGES: ix, 95

ABSTRACT:

Graft versus Host Disease (GvHD) is one of the main complications patients face after receiving a bone marrow transplant.[1] Between 40-60% of bone marrow transplant recipients develop GvHD, with consequent systemic inflammation/fibrosis, reduced quality of life, graft failure, and mortality.[2] We have previously demonstrated that donor-derived C5 is involved in the initiation and propagation of GvHD. Current approaches to inhibition of C5 share a serious flaw of indiscriminately blocking production of a mediator that is crucial for host defense. Targeted therapies to block C5 in specific cells, or anatomical sites, are the only way in which to achieve therapeutic benefit without compromising host defenses. Three lentiCRISPR v2-dCas9 gene editing viral constructs were created to selectively cleave the complement C5 gene, at three different sites. Our objective was to knockout complement C5 function in infected donor BM cells in a GVHD mouse model. Each of the three lentiCRISPR plasmids was separately co-cultured with PMDG2 and PSPAX2, in human embryonic kidney (HEK) 293T cells. Resultant viral particles were able to transfer the Cas-9 endonuclease gene into donor BM cells in vitro with a transduction efficiency of 52%. Treated donor BM cells were then retro-orbital injected into irradiated recipient mice. Control mice were transplanted following the same protocol excluding the lentiCRISPR treatment of BM. The lentiCRISPR treatment group demonstrated significantly lower total airway resistance ($p = 0.05$) and higher lung compliance ($p = 0.014$) when compared to the control group. When compared to the saline treated group however the lentiCRISPR group showed significantly higher total airway resistance ($p = 0.004$) and significantly lower lung compliance ($p = 0.014$). These results taken together suggest a possible reduction in GvHD severity in mice that received the lentiCRISPR treatment. This study can serve as a starting point for the development of this novel treatment of GvHD.

Acknowledgements

These past 19 months have been an educational journey on science, life and the vitality of building a strong support network. I learned life lessons that will stay with me long after I am finished at McMaster and I am certain they will help me overcome any future challenges. I want to start by thanking my supervisor, Dr. Mark Larché for giving me the opportunity to be a part of his lab as a master's student. You provided all the resources a student could need to succeed and I am grateful. I also want to thank my committee members, Dr. Matthew Miller, Dr. Kjetil Ask and Dr. Todd Hoare for all of their feedback, guidance and insights. Without your guidance my research project would not have been possible. Believe me when I say your suggestions were invaluable. To my lab mates, Cheryl, Tom, Lesley and Elena, I want to say thank you for showing me the ropes of the lab and how to find and utilize the available resources.

I want to give a big thank you to Dr. Bramson for his crucial suggestion to use lentiviral delivery and an even bigger thank you to Dr. Samuel Workenhe with whose help the lentiCRISPR vectors were developed. I have been privileged to meet so many inspiring colleagues, that have helped me along the way, and I want to thank as many as I can. To Peter Zhang, who was always willing to take time out of his day to show me procedures or just be a friend to bounce ideas off of. To Dr. Ali Akbari, in Dr. Hoare's lab, who generated the polymer delivery systems tested for the CRISPR/Cas9 plasmid. To Dr. Karen Mossman's lab, especially Susan Collins, who taught me the art of nucleofection. To Arya Afsahi, who taught me electroporation. Finally to Dr. Anna Dvorkin who contributed the data on C5 production of different cell types, effectively shaping the direction for the project by providing us with the evidence required to select a cell target.

A sincere thank you to Dr. Jewel Imani and Melissa MacDonald. Jewel built the foundation of this project throughout his PhD and was always willing to teach me the skills that took him years to perfect. Melissa played a vital role in this project as well. She taught me how to work with animals, from the very basics of handling them to intricacies of ventilation and proper tissue collection. Her impeccable organizational skills and unwavering dedication to her work are traits I greatly admire and will strive to emulate in my own life. I have learned a lot from both of you and I am eternally grateful for your time, patience and the knowledge you have given me.

I want to thank the amazing friends I made Joanna, Danielle and Caroline. You were the best support system I could have asked for. Joanna was a master of laboratory techniques and was always willing to share her knowledge. Caroline's passion for statistics and patience in teaching made learning from her a fun experience. Finally Danielle's infectious positive attitude kept us smiling. I am glad I had the chance to meet you all.

Finally I want to thank my parents and brother, who are always supportive, encouraging and taught me how to persevere.

Table of Contents

Abstract ii

Acknowledgements iii

Table of contents v

List of supplementary figures vii

List of figures vii

List of tables ix

List of abbreviations

Declaration of academic achievement

1.0 Background 1

Allogeneic hematopoietic stem cells transplant 1

Graft Versus Host Disease 1

Pathophysiology of GvHD: Acute and Chronic 3

Central tolerance 5

Regulatory T lymphocytes 6

B lymphocytes and autoantibody formation 7

Fibrosis 8

The complement system 9

The role of C5 in normal immune function vs in GvHD 11

Lack of current effective treatment methods 14

CRISPR gene editing 16

Retroviruses and lentiviral delivery of nucleic acids 17

Lentiviral vectors 19

Second generation vs third generation lentivirus 20

LentiCRISPR plasmids 21

LentiCRISPR delivery of genomic segments into bone marrow 22

2.0 Methods and Results 24

Hematopoietic stem cells are a promising target for genetic modification of C5 24

Design of complement component C5 specific CRISPR/Cas9 knockout plasmid 26

Lipofectamine produces high transfection rates in HEK 293T cells with CRISPR/Cas9 knockout plasmid 27

Nucleofection of murine bone marrow with CRISPR/Cas9 plasmid results in low transfection rate 28

Electroporation of murine bone marrow with CRISPR/Cas9 plasmid results in low transfection rate .. 32

Polymer delivery of CRISPR/Cas9 plasmid to murine bone marrow results in low transfection rate 35

GvHD is developed following an allogeneic-whole bone marrow transplant in murine model 43

Murine model of GvHD 43

There was no statistically significant difference in total airway resistance levels between historical C5 competent mice and current C5 competent mice termed control mice in this study 44

There was no significant difference in post-transplant survival rates between mice that received $1x10^6$ or $2x10^6$ BM cells in GvHD murine model 46

There was no significant difference in total airway resistance or lung compliance between mice that received $1x10^6$ or $2x10^6$ BM cells in GvHD murine model 47

There was no observable difference in post-transplant body condition between mice that received $1x10^6$ or $2x10^6$ BM cells in GvHD murine model 48

Rodent mechanical ventilator assessed lung airway physiology suggests development of GvHD in murine model 49

LentiCRISPR vectors were developed to knockout expression of C5 in murine bone marrow cells as a potential treatment for GvHD 56

Co-transfection of lentiCRISPR vectors, PMDG2 and PSPAX2 vectors to produce lentiviral particles in HEK 293T cells 57

Working concentration of 0.5 μg/ml of Puromycin is appropriate for selection of transduced murine bone marrow cells 58

In vitro lentiCRISPR treatment of BM cells produces high transduction rates 59

LentiCRISPR vector generated knockout of C5 in donor bone marrow may be a promising potential treatment for GvHD 61

Murine model of GvHD transplanted with lentiCRISPR treated bone marrow leads to reduction in disease severity 62

Histologically assessed changes in airway morphology imply decreased disease severity in lentiCRISPR treated BM recipient mice 70

Alternate statistical analysis of ventilator derived data for lentiCRISPR group demonstrated reduction in disease severity in lung compliance but not in total airway resistance 71

3.0 Discussion and Limitations **76**

4.0 Appendix **84**

5.0 References **91**

List of Supplementary Figures

Supplementary Figure 1: LentiCRISPRv2 vector

List of Figures:

Figure 1: Cell types that express complement component C5 in humans

Figure 2: Cell types that express complement component C5 in mice

Figure 3: Chitosan:TPP polymer tested

Figure 4: CMCS:TPP polymer tested

Figure 5: Components of POEGMA:DMAEMA polymer tested

Figure 6: BM cell transfection with CRISPR/Cas9 plasmid via Chitosan:TPP 5/1.25 mg/ml

Figure 7: BM cell transfection with CRISPR/Cas9 plasmid via Chitosan:TPP 2.5/0.6 mg/ml

Figure 8: BM cell transfection with CRISPR/Cas9 plasmid via Control (H2O + Plasmid)

Figure 9: BM cell transfection with CRISPR/Cas9 via POEGMA:DMAEMA 10:90%

Figure 10: BM cell transfection with CRISPR/Cas9 via POEGMA:DMAEMA 25:75%

Figure 11: Comparison of total airway resistance of historical C5+ group and control group

Figure 12: Body condition of recipient mice of 1 million vs 2 million BM cells

Figure 13: Comparison of total airway resistance of trial, C5 deficient and saline groups

Figure 14: Comparison of lung compliance for trial, C5 deficient and saline groups

Figure 15: Comparison of total airway resistance of lentiCRISPR, saline and control groups

Figure 16: Comparison of lung compliance for lentiCRISPR, saline and control groups

Figure 17: Histology of murine lungs of lentiCRISPR and control mice

Figure 18: Adjusted data comparison of lung compliance for lentiCRISPR, saline and control

Figure 19: Adjusted data comparison of total airway resistance of lentiCRISPR, saline and control groups

Figure 20: Total airway resistance comparison for 4x lentiCRISPR, saline and control groups

Figure 21: Lung compliance comparison for 4x lentiCRISPR, saline and control groups

List of Tables:

Table 1: CRISPR/Cas9 sgRNA Sequence

Table 2: Transfections of HEK 293T Cells with CRISPR/Cas9 Plasmid via Lipofectamine

Table 3: Optimization of nucleofection for resting murine BM cells with Human CD34+ kit

Table 4: Optimization of nucleofection for resting murine BM cells with Human CD34+ kit

Table 5: Optimization of nucleofection for resting murine BM cells with Mouse Embryonic Stem Cell kit

Table 6: Optimization of nucleofection for resting BM cells with Human Mesenchymal Stem Cell kit

Table 7: Optimization of electroporation for resting murine bone marrow cells

Table 8: Optimization of electroporation for resting murine bone marrow cells

Table 9: CRISPR/Cas9 Plasmid Transfection of Murine BM via Polymer Delivery

Table 10: CRISPR/Cas9 Plasmid Transfection of Murine BM via Polymer Delivery

Table 11: CRISPR/Cas9 Plasmid Transfection of Murine BM via Polymer Delivery

Table 12: Mann-Whitney test for total airway resistance between historical C5+ group and control group

Table 13: Chi-Square test for survival rates of recipients of 1 million vs 2 million BM cells

Table 14: Mann-Whitney test for total airway resistance of recipients of 1 million vs 2 million BM cells

Table 15: Mann-Whitney test for lung compliance of recipients of 1 million vs 2 million BM cells

Table 16: Kruskal-Wallis test for total airway resistance of Trial, Saline, C5 Deficient groups

Table 17: Mann-Whitney test for total airway resistance of Trial and C5 Deficient groups

Table 18: Mann-Whitney test for total airway resistance of Trial and Saline groups

Table 19: Kruskal-Wallis for Compliance of Trial, Saline, C5 Deficient

Table 20: Mann-Whitney test for lung compliance of Trial (n=12) and Saline (n=5) groups demonstrated statistically significant difference between the groups (p = 0.002).

Table 21: Mann-Whitney test for lung compliance of Trial (n=12) and Saline (n=5) groups demonstrated statistically significant difference between the groups (p = 0.002).

Table 22: LentiCRISPR sgRNA Sequences

Table 23: Puromycin Kill Curve of Wildtype Untreated Murine Bone Marrow

Table 24: Puromycin Selection of LentiCRISPR Treated Murine Bone Marrow

Table 25: Kruskal-Wallis Test for total airway resistance of lentiCRISPR, saline, control

Table 26: Mann-Whitney test for total airway resistance of lentiCRIPSR and control groups

Table 27: Mann-Whitney test for total airway resistance of lentiCRIPSR and saline groups

Table 28: Mann-Whitney test for total airway resistance of saline and control groups

Table 29: Kruskal-Wallis test for lung compliance of lentiCRIPSR, saline and control groups

Table 30: Mann-Whitney test for lung compliance of lentiCRISPR and control groups

Table 31: Mann-Whitney test for lung compliance of lentiCRISPR and saline groups

Table 32: Kruskal-Wallis test for adjusted lung compliance of lentiCRISPR, saline and control

Table 33: Mann-Whitney test for adjusted lung compliance of lentiCRISPR and control groups

Table 34: Mann-Whitney test for adjusted lung compliance of lentiCRISPR and trial groups

Table 35: Mann-Whitney for adjusted total airway resistance of lentiCRISPR and control groups

Table 36: Kruskal-Wallis test for total airway resistance of 4x lentiCRIPSR, saline and control

Table 37: Mann-Whitney test for total airway resistance of 4x lentiCRISPR and control groups

Table 38: Mann-Whitney test for total airway resistance of 4x lentiCRISPR and saline groups

Table 39: Kruskal-Wallis test for lung compliance of 4x lentiCRIPSR, saline and control groups

Table 40: Mann-Whitney test for lung compliance of 4x lentiCRISPR and saline groups

Table 41: Mann-Whitney test for lung compliance of 4x lentiCRISPR and control groups

List of Abbreviations and Symbols:

aGvHD – acute Graft versus Host Disease

cGvHD – chronic Graft versus Host Disease

BM – bone marrow

C3a – complement component 3 subunit a

C5 – complement component 5

C5a – complement component 5 subunit a

C5aR – C5a receptor

C5b – complement component 5 subunit b

DC – dendritic cell

HLA – human leukocyte antigen

MMF – mycophenolic mofetil

APC – antigen presenting cell

C3aR – C3a receptor

mHA – minor histocompatibility antigens

BAFF – B cell activating factor

C2a – complement component 2 subunit a

C9 – complement component 9

C4b – complement component 4 subunit b

C6 – complement component 6

IL-4 – interleukin 4

IL-5 – interleukin 5

IL-13 – interleukin 13

CCL3 – macrophage inflammatory protein 1α

CCL2 – monocyte chemoattractant protein 1

IgM – immunoglobulin M

IgG – immunoglobulin G

C1q – complement component

MBL – mannose binding lectin

Allo-HSCT – allogeneic hematopoietic stem cell transplant

LPS – lipopolysaccharide

CD34+ cells – hematopoietic stem cells

CYA – cyclosporine A

TAC – tacrolimus

CRISPR – Cas9 nuclease from the microbial clustered regularly interspaced short palindromic repeats

Cas9 – CRISPR associate protein 9

RNA – ribonucleic acid

DNA – deoxyribonucleic acid

NHEJ – non-homologous end joining pathway

HDR – homology-directed repair pathway

Indel – insertion/ deletion

TALENs – transcription activator-like effector nucleases

ZFNs – zinc-finger nucleases

PAM – protospacer adjacent motif

ENV – envelope glycoprotein

MA – matrix protein

RT – viral reverse transcriptase

NC – nucleocapsid

CA – capsid

IN – integrase

PR – protease

HSC – hematopoietic stem cells

HSCT – hematopoietic stem cell transplant

Treg – T regulatory cell

MAC – membrane attack complex

MHC – major histocompatibility complex

mHC – minor histocompatibility complex

Gag – group antigens

LTR – long terminal repeat

Nef – negative factor

Vpu – viral protein U

Vif – virion infectivity factor

Rev – RNA-binding protein

HIV – human immunodeficiency virus

Tet – tetracycline

Cre – carbapenem-resistant Enterobacteriaceae

VSV-G – vesicular stomatitis virus G protein

CMV (promoter) – cytomegalovirus

RSV (promoter) – respiratory syncytial virus

sgRNA – single guide RNA

Vegfa – vascular endothelial growth factor

Hc – hemolytic complement

PBS – phosphate buffered saline

RBC – red blood cell

RO – retro-orbital

Th1 – T helper cell type 1

Th2 – T helper cell type 2

Declaration of academic achievement

I performed the necessary procedures and tasks for Figure 12 through Figure 21 with Melissa MacDonald, our lab technician, as an assistant. Data for historical groups, such as in Figure 11, was provided by Dr. Jewel Imani. I personally performed testing of lentiCRISPR vectors both in vitro and in vivo, the vectors were provided by Dr. Samuel Workenhe.

Dr. Anna Dvorkin performed the analyses needed to create Figure 1 through Figure 2. For Figure 3 through Figure 5, I worked alongside Dr. Ali Akbari from Dr. Todd Hoare's lab. I personally performed all the necessary procedures to produce Figure 6 through Figure 10, the polymers tested were provided by Dr. Ali Akbari.

1.0 Background

Allogeneic hematopoietic stem cell transplant

An allogeneic hematopoietic cell transplant is a bone marrow transplant from a genetically similar but non-identical donor. It is used as a treatment and can be potentially curative for an array of different hematological malignancies, such as chronic leukemias and aplastic anemia [3]. The donor is normally a brother or a sister of the patient but it can be from an unrelated individual as well. Donors are normally selected based on several parameters including HLA typing, conditioning regimens and supportive care. Previously this procedure was seen as an end stage rescue attempt once the disease progressed to its late stages [3]. Over the course of the last decade or so there has been an increasing trend of applying this treatment earlier on based on growing evidence in the literature that recipient outcomes are dependent on timing [4]. The increase in prevalence of this procedure creates an even greater need for developing effective post-transplant treatment regimens to ensure graft and patient health.

Graft versus Host Disease

Graft versus Host Disease is a multisystem disorder and a common complication following allogenic hematopoietic stem cell transplant (HSCT). It affects approximately 40–60% of all patients that receive a bone marrow transplant and survive the first 100 days [2]. In GvHD the immune cells of the donor, in the donated graft, recognize the recipient tissues as foreign and mount an immunological reaction, initiating the disease state in the transplant recipient.

There are two diagnostic forms of GvHD, acute (aGvHD) and chronic Graft versus Host Disease (cGvHD). The two differ in both time of onset and in the tissues affected. The symptomatology associated with the two distinct form of GvHD is commonly used as the cut off

between acute and chronic variants of the disease [5]. Although, classic cGvHD may present at any time following the transplant it does not share any of the diagnostic symptoms of acute GvHD.

Patients with aGvHD commonly develop maculopapular rash, persistent nausea and/or emesis, abdominal cramps and diarrhea, and an increase in serum bilirubin. In comparison cGvHD presents with skin manifestations resembling scleroderma, dry oral mucosa with ulcerations and sclerosis of the gastrointestinal tract, as well as an increase in serum bilirubin [5].

cGvHD remains poorly characterized and the mechanisms of onset are still unclear. Although, there have been improvements made in both the understanding and treatment of the disease, according to Gyurkocza B. et al (2010) the overall incidence of cGvHD has remained mostly unchanged over the last 25 years. This steady or possibly increasing incidence rate may be attributed to the improvements in survival and longevity of recipients post-transplant [6].

There is still a lack of clear consensus on whether cGvHD is a progressive state of aGvHD or should be given its own independent disease status. This is mainly fueled by the physiological manifestations of the disease such as dermal fibrosis, which highly resemble those of classic autoimmune diseases such as systemic sclerosis scleroderma [6].

The current first-line treatment of chronic GvHD is comprised of corticosteroids. For those patients that are unresponsive to steroids a popular second-line treatment drug includes mycophenolic mofetil (MMF), an immunosuppressive agent, for treating chronic GvHD. However, in a study by Martin PJ et al. (2009) MMF therapy was shown to have no beneficial effect on patient outcomes in transplant recipients with resulting chronic GvHD [7], suggesting a serious need for new and effective treatment options.

Although cGraft versus Host Disease is generally considered to be a T-cell mediated condition, the literature suggests that antigen presenting cells (APCs) play a key role in priming alloreactive donor T cells to induce the onset of GvHD [8]. APC derived complement components are an important mechanism for T cell activation and, as suggested by Kwan WH et al. (2012), lead to an exacerbation of GvHD outcomes [9]. In their study, Kwan et al. (2012), demonstrated that following total body irradiation there was a measurable upregulation and activation of alternative pathway complement components via host APCs, which in turn lead to an increase in splenic and organ-infiltrating T cell expansion. Their key finding, however, included that T cells lacking in a C3a or C5a receptor had a weak response in the recipient and exhibited a more limited ability to induce GvHD. In another study by Hung Nguyen J et al. (2015), complement C3a and C5a receptors were targeted to control onset of acute GvHD in a murine model [8]. In the study the role of C3aR and C5aR regulated by APC function was evaluated as a means of prevention for the onset of acute GvHD. The results demonstrated that a host deficiency of C3aR and C5aR lead to a significant decrease in the incidence of aGvHD when compared to wildtype murine recipients. Overall, this data suggests a strong link between C3aR and C5aR, as well as C3a and C5a producing APCs, and the induction of GvHD.

Pathophysiology of GvHD: Acute and Chronic

Early murine models of Graft versus Host Disease aided in furthering our understanding of the key cells that mediated the disease state in HSCT recipients. One such model, developed by Billingham et al (1966), lead to the recognition that the immunological response in GvHD is donor T cell derived, wherein the donor T cells recognize host tissues as foreign and consequently mount an attack [10]. This observation lead to the establishment of the basic requirements for development of GvHD post-transplant. Those included immunologically active T cells being

present in the donated graft, the expression of host antigens absent in the donor, and finally a lack of effective immunological responses in the recipient leaving them unable to eliminate the graft [10].

Although advancements have been made in increasing donor and recipient compatibility through HLA typing, for example, the patient may still develop GvHD due to minor histocompatibility antigens (mHA) [11]. These constitute peptides that can be presented in combination with MHC on the surface of antigen presenting cells and are capable of inducing a T cell response. These general findings indicate T cells as the primary cellular instigator of chronic GvHD however, other cells may play important complementary roles. B cells are one such example with previous studies describing autoantibodies in cGvHD, directed against numerous mHA [12]. Understandably a number of subsequent studies focused the effects of anti-B-Cell agents as possible treatment options in cGvHD. In one such study, by Sarantopoulos et al (2007), it was noted that dysregulation of B cells may be associated with the chronic disease onset and its persistence [13].

In acute GvHD the host APCs, in particular dendritic cells, present alloantigens to alloreactive cytotoxic T cells which in turn leads to host tissue damage. Such damage sustained to gastrointestinal mucosa for example leads to the upregulation of the innate immune system [14]. These innate immune mechanisms play an integral although different role in the pathophysiology (initiation and propagation) of both acute and chronic forms of Graft versus Host Disease. However, there is a strong necessity for further research into the pathophysiology of the chronic form of GvHD, which still remains obscure, to help us develop effective treatment.

Currently there is no one agreed upon theory of disease development or progression for cGvHD. The three currently prevailing theories are central tolerance dysfunction, regulatory T cell derived and B cells and antibodies, with fibrosis being a major sign of the disease state.

Central Tolerance Dysfunction

Previous literature has proposed that a disruption of the normal processes of immune tolerance (death by neglect, positive selection, and negative selection) may play a role in onset of cGvHD [15]. A possible explanation, put forth by Kishimoto et al. (2001), suggests that during the reconstitution of the immune system, post-transplant, damage may be caused to the thymic epithelium of the host, in turn leading to dysregulation of central tolerance mechanisms [15].

Positive Selection: In the thymic cortex immature double-positive (CD4+/CD8+) T cells are presented with self-antigens by thymic cortical epithelial cells. The T cells that bind with low affinity to MHC class I and MHC class II molecules receive survival signals and proceed to the next stage of maturation [16].

Death by Neglect: Double-positive (CD4+/CD8+) immature T cells that bind with a lower affinity to MHC I and II fail to receive the survival signals and die via apoptosis [16].

Negative Selection: Active induction of apoptosis in single-positive T cells that are strongly autoreactive when they encounter self-peptides on APCs in the thymic medulla [16].

The balance of positive and negative selection is crucial once these naïve T cells enter the periphery and encounter self-antigen/MHC complexes. In pro-inflammatory environments this balance may be disrupted, in which case peripheral tolerance mechanisms would be crucial in regulating graft versus host disease [15].

In a paper by Dutt et al. (2007), it was suggested that T helper cells that arise from donor stem cells possibly mediate the progression from aGvHD to cGvHD. This would indicated that T cell education during the reconstitution of the immune system (post-transplant) would be crucial in pathogenesis of the disease [17].

During the onset of cGvHD, central tolerance failure could lead to symptomatology of the disease to resemble that of an autoimmune disease [15]. A natural step would be to study the thymus for possible causation of disease onset and presentation. However, a study by Zhang et al (2006), demonstrated that the host thymus was not required for cGvHD onset [18]. Instead dormant autoreactive T and B cells in the donor graft could be activated leading to the onset of cGvHD.

Regulatory T lymphocytes

The relationship between regulatory T cells (Tregs) and cGvHD has been outlined by a number of studies. Although, results have been contradictory to date. Some studies, such as the one conducted by Zorn et al. (2005), have shown a decline in Treg numbers following the onset of cGvHD [19]. Others studies have shown instead an increase in peripheral blood Treg numbers in patients with cGvHD, which decreased following the resolution of the disease, suggesting that Treg deficiency would not be responsible for the onset of cGvHD [20]. The overall literature on regulatory T cells and their relationship to cGvHD suggests that Tregs help to suppress cGvHD. Although the mechanisms of suppression still remain elusive, several cytokines and cells have been identified as mediator for Treg action including plasmacytoid dendritic cells [21].

The relationship between regulatory T cells and cGvHD has important clinical implications when it comes to developing treatment regimes. Previous studies have demonstrated that in animal models a donor transfer of Tregs along with administration of glucocorticoids can act to prevent

the onset of cGvHD following a HCT [22]. In a contradictory study however, Zhang et al. (2006), demonstrated that peripheral tolerance may be more critical to prevention and control of cGvHD than Tregs [18]. In fact their study suggested that donor Tregs might abolish the efficacy of peripheral tolerance mechanisms on cGvHD. Further research is clearly needed in order to create a holistic understand of the role of regulatory T cells in cGvHD.

B lymphocytes and Autoantibody Formation

As a whole, previous literature on the subject of cGvHD has heavily focused on donor T lymphocytes and the development of different treatment approaches to suppressing or decreasing the function of these cells. A key pivotal study by Ratanatharathorn et al. (2000) drew the focus to B lymphocytes as a possible contributor to disease development and propagation [23]. The study observed the effect of rituximab, a B cell depletion therapy, and suggested that complex interactions between B and T lymphocytes were responsible for disease onset. Numerous studies since then have noted the formation of autoantibodies in patients with GvHD, however, the mechanisms of action still remain unclear [24]. A particular example was conducted by Svegliati et al. (2007), who observed the formation and presence of autoantibodies in patients with cGvHD and a lack there of in patients not suffering from cGvHD [25]. The clinical presentation of B cell activity in cGvHD can be observed by monitoring B cell activating factor (BAFF) serum levels. In a study by Sarantopoulos et al. (2007), the increase in plasma levels of BAFF, 6 months post-transplant, was found to be a predicting factor for the development of cGvHD in asymptomatic patients [13]. As seen in studies attempting to establish the efficacy of rituximab and other B cell

depletion therapies as treatments for graft versus host disease, B lymphocytes are a promising treatment target [26].

Fibrosis as a sign of GvHD

cGvHD induced fibrosis affects multiple organ systems including the skin, liver, kidneys and lungs [27]. Dermal symptoms can be observed as a severe mononuclear inflammatory cell infiltrate, irregular acanthosis, hyperkeratosis, dermal fibrosis and sclerosis, and general deteriorative changes in the epidermal-dermal junction [27]. Multiple studies on the formation of fibrosis in cGvHD have revealed a link between type 2 polarized immune responses (T2 effector cells) and the development of fibrosis. In one murine model used by Nikolic et al. (2000), it was found that type 2 immune responses were a necessity for the initiation of cutaneous GvHD [28]. A different study by Hillebrandt et al. (2005), outlined the possible role complement component C5 may play in liver fibrosis in mice and humans with cGvHD, where they found that liver fibrosis was modified with dose-dependent administration of C5 [29]. Although, complement components C5-C9 deposits have been described in the skin, liver, lungs and kidneys of murine models of cGvHD, the deposition mechanisms and consequences remain obscure [30].

Mounting experimental evidence strongly suggests that following an allo-HSCT, the preferential expansion of T helper type 2 cells is connected with the development of cGvHD in both mice and humans [31]. In fact the phenotype of T helper cells that develops during this response may be critical to the development of fibrosis and to the progression of the disease. Specifically development of the CD4+ Th2 cell as opposed to the Th1 cell response is indicative of fibrogenesis [31].

Development of connective-tissue deposits due to the Th2 response also involves several cytokines including IL-4, IL-5 and IL-13. The differences between the preferential response, Th1 or Th2, suggests that chronic inflammation does not necessarily correlate with the induction of connective-tissue deposits [15].

The CC-chemokine family has been shown to have a key regulatory role in the development of fibrogenesis. In fact macrophage inflammatory protein 1α (CCL3) and monocyte chemoattractant protein 1 CCL2 are in a sense pro-fibrotic mediators via their attraction action of mononuclear phagocytes [15]. In a study by Yoon et al. (2010), it was found that pravastatin attenuated murine cGvHD by blocking the influx of effector cells, as well as acting to down regulate levels of monocyte chemoattractant protein, which resulted in reduced collagen synthesis [32].

The Complement System

Complement is an important part of innate immunity and serves as a bridge connecting innate immunity to acquired immunity. The complement system is made up of a series of proteins that interact with one another [33]. The large majority of those proteins are synthesized in the liver and are present in the body as inactive precursors. One key role for complement is its facilitation of inflammatory responses through a consecutive enzyme cascade. This enzyme cascade then results in the elimination of foreign matter via pathogen recognition, opsonisation and lysis [34].

There are three independent pathways of complement activation. They include the classical pathway, an alternative pathway and a lectin pathway. The three differ in the way in which they activate the complement cascade [33]. The first step in the classical pathway is the formation of IgM or IgG antigen/antibody complexes that then bind to C1q, the initial protein in the complement

cascade. This leads to the activation of serine proteases and the formation of C3 convertase, which cleaves C3 into the inflammatory cell recruiter C3a and C3b, which contributes to the formation of the C5 convertase. The classical pathway can also be initiated by viral proteins, apoptotic cells and amyloid [35]. Through the alternative pathway however, it was discovered that for activation to occur interaction with antibodies was not necessary, in fact bacteria, yeast or damaged cells could bind to complement system components directly [33]. More importantly the alternative pathway is not specifically a new method of activation of the complement system but rather an inability to regulate the continuous, low levels of C3 convertase being produced in the body [33]. The mannose binding lectin (MBL)/ MBL-associated serine protease pathway of complement activation is initiated by collectins, mannose binding lectin and ficolin. These lectin complexes bind to foreign carbohydrates and activated the complement pathway through MBL-associated serine proteases [36].

All three complement activation pathways converge to a common pathway that leads to the activation of complement component C3. C3 activation then leads to the formation of numerous bioactive molecules, including C5a, and finally to the formation of the membrane attack complex (MAC) on target cells [35]. Although, the complement system is a key mediator in inflammatory responses it also exhibits anti-inflammatory roles. For example complement components bind to immune complexes on damaged cells and aid in their removal [33]. The majority of the complement proteins remain in an inactive state as precursors and are only activated at the site of inflammation. The rapid association and dissociation of the complement components is a means of regulating the complex cascade [35]. Furthermore, the different proteins that make up the complement system are non-covalently associated which increases the complexity of the activation cascade and its regulation.

Role of C5 in normal immune function vs. in GvHD

In a healthy individual complement component C5, being a part of the complement cascade, plays an integral role in the body's natural defenses against infection and inflammation. Through activation of the complement system both increased recruitment and phagocytosis by innate immune cells (opsonisation) leads to lysis of the target cells [34]. In this process complement component C3 is the initial step where all activation pathways converge. During this initiation step C3 is cleaved into C3a and C3b. C3b then goes on to form a part of the C5 convertase along with C4b/C2a. The C5 convertase then cleaves C5 into two parts, C5a and C5b. C5b is of particular importance in its interaction with C6 – C9, which together form the C5b-9/Membrane attack complex (MAC) [35]. The MAC complex then inserts itself into the membrane of the target cells and forms a pore, this disruption in the cell membrane's function then leads to cell lysis. C5a on the other hand has a multitude of different actions dependent on the cell type it is interacting with [46]. It is important as an enhancer of recruitment, activation and phagocytosis by innate immune cells, chemotaxis, stimulation of the release of granular enzymes and histamine, vasodilation and the stimulation of cytokine production [34].

Although complement C5 plays an integral role in the normal function of our immune system, it has also been identified as a key mediator and intermediate in the pathogenesis of multiple diseases including solid organ transplant rejection and ischemia reperfusion injury following the transplant, graft versus host disease, rheumatoid arthritis and others [37, 38]. Donor-derived C5 was also implicated in the induction of GvHD based on the data from a previous, unpublished murine study of pulmonary GvHD, from our lab. The study demonstrated that transplantation of C5 competent mouse bone marrow and spleen cells into C5 competent recipient mice induced lung GvHD symptoms, while C5 deficient donor cells did not.

One of the main sites of complement component production is the liver, however, other cell types, including blood cells have been shown to secrete and release a variety of complement proteins, their regulators and their receptors. Specifically when considering an allo-HSCT, monocytes/macrophages and dendritic cells have all been shown to produce significant quantities of C5 [39, 40]. The production of these complement components by these cells has been shown to play a key role in transplant-associated pathologies, independently of host-derived complement components synthesized by the liver. A study by Kwan et al (2012) implicated APC derived C3a and C5a as regulators of T cells immunity in a murine GvHD model, wherein they observed that APC produced C3a and C5a exacerbating GvHD outcomes and caused splenic and organ-infiltrating T cell expansion. In their study T cells that lacked the C3a or C5a receptors presented with a weaken response and an inability to initiate GvHD [9].

In a different study by Nguyen et al. (2015), the researchers attempted to target host complement C3a and C5a receptors to control the onset of aGvHD in a murine model [8]. In their study it was observed that a lack of C3a/C5a receptors on host T cells lead to significant decrease in incidence of aGvHD and that the ameliorated GvHD in these C3a/C5a receptor deficient mice was associated with a reduction in donor T-cell activation, survival and Th1 differentiation. It also resulted in increased regulatory T cell generation. They also found that the expression of C3a and C5a receptors on the recipients's antigen presenting cells was primarily responsible for donor T cell response and pathogenicity.

Since dendritic cells, in comparison to other APCs, have a superior ability to take up and express antigen and produce pro-inflammatory cytokines that polarize alloreactive T cell, they are a natural choice when considering development of treatments for GvHD [9, 41].

Furthermore multiple subsets of dendritic cells including Langerhan's cells, myeloid DC, plasmacytoid DC and monocyte-derived DC, express a range of complement components, including C5, at high levels both at rest and following activation with LPS [39, 40]. This makes these APCs a logical target when attempting to study the effects of cell targeted complement component C5 depletion in vitro.

In vivo studies of the role of complement component C5 in GvHD however, may benefit from a broader cell target due to the frequent turnover rate of APCs. APC targets outlined above, are derived from a common lineage, stemming from hematopoietic stem cells in bone marrow [42]. These hematopoietic stem cells can differentiate into one of two lineages, the myeloid lineage and the lymphoid lineage [43]. Cells that enter the myeloid lineage can then further differentiate into megakaryocytes, erythrocytes, mast cells, and myelobasts, the latter of which gives rise to monocytes. Monocytes then differentiate into dendritic cells and macrophages [43, 44]. The lymphoid lineage on the other hand gives rise to small lymphocytes and natural killer cells. Both B and T lymphocytes originate from the small lymphocyte progenitors. These facts taken together lead to the conclusion that hematopoietic stem cells are a reasonable broad cell target when attempting to alter C5 levels produced by APC such as dendritic cells, macrophages and B cells, involved in GvHD. Another key factor to consider when choosing an appropriate cell target for in vivo experimentation is the standard life cycle of the cells in question. In general dendritic cells turnover rates are tissue dependent but they have been shown to have a half-life as short as 1.5-2.9 days in mice [45]. When considering macrophage viability in the body a substantial turnover

for tissue resident macrophages can be expected to occurs between 0 – 21 days [45, 46]. Therefore any genetic alteration that was applied to mature DC cells or macrophages in vivo would be lost within 21 days, as these genetically modified APCs follow their natural life cycle and are replaced with newly derived APC from the bone marrow. Since the APCs, responsible for a significant amount of the non-hepatocyte-derived production of component C5 in the body, are of hematopoietic stem cells (CD34+ cells) descent, CD34+ cells would be a natural target when considering C5 depletion in animal models.

Lack of current effective treatment methods

During the last decade chronic GvHD has emerged as one of the most troubling complications following a bone marrow transplant [47, 48]. The disease's resemblance to autoimmune disorders makes it even more difficult to diagnose and treat early on. The manifestations of the disease normally appear within the first year following an allo-HSCT. This may be due to the gradual weaning of immunosuppressive medications [49]. Other possible complications following an allo-HST include eczema, iron overload, hypothyroidism, and infections all of which could be misdiagnosed, and therefore improperly treated, as chronic GvHD [48, 50]. Once properly diagnosed however, chronic GvHD treatment can begin. Currently treatments focus on alleviating symptoms rather than being curative. The long-term goal when it comes to treating GvHD still remains immunological tolerance and the ability to cease all immunosuppressive medications without causing renewed or exacerbated disease manifestations in the patient. Unfortunately, no current approaches are able to provide such an outcome.

Those patients that fit the moderate to severe diagnostic criteria for chronic graft versus host disease are treated with systemic therapy for at least one year. Patients that fall under the high-

risk diagnostic profile due to concomitant thrombocytopenia or hyperbilirubinemia for example, but present with less severe systems are equally treated with systemic therapy. Those that present with mild symptoms are often treated with topical therapies alone [49].

Primary systemic treatment for chronic GvHD consists of corticosteroids. Normally treatment is initiated with prednisone, an oral corticosteroid, at 0.5 to 1 mg/kg per day [50]. It can be administered with calcineurin inhibitors such as cyclosporine A (CYA) or tacrolimus (TAC), depending on the patient's need for immunosuppression. However, efficacy of this treatment plan or a standardized dosing regimen have not yet been established and the side-effects of systemic corticosteroid treatment are severe [49, 51]. Patients experience a wide range of side-effects affecting quality of life including hypertension, myopathy, diabetes, bone loss, toxicity, and are at an increased risk of contracting infections [50]. Often combinational therapy with immunosuppressive medications, such as mycophenolic mofetil (MMF) and thalidomide, are favored when systemic corticosteroids must be used over a longer period of time in an attempt to reduce toxicity. However, results from randomized trials indicated no significant benefit to the initial treatment of chronic GvHD [52]. Furthermore the appropriate management of chronic GvHD is intensive and consistent recalibration of immunosuppressive treatments is necessary in order to avoid over- or under-treatment of the patient. Simply the fact that between 50-60% of patients with cGvHD require a secondary systemic treatment within two years of initiating the first systemic treatment is indication enough that the efficacy of the initial line of treatment is not satisfactory [50].

Unfortunately, adding a secondary systemic treatment does not provide renewed hope, especially since there is currently no consensus and few guidelines for what the optimal secondary agent should be [50]. At that point patients rely on their physician's experience, the drug's ease of

use, need for monitoring and risk of toxicity [49]. Even though chronic GvHD is associated with a lower relapse rate, most likely due to the graft-versus-leukemia effects, it is still associated with immune dysfunction and a risk of infection and reduced quality of life [53]. Clearly new and effective treatment approaches are a necessity if we hope to improve the outcomes and the quality of life of those with chronic GvHD.

CRISPR Gene Editing

One possible technology that can be exploited to meet this need is the CRISPR/Cas9 gene editing system. The medical and scientific applications and implications of genome editing are enormous. The current sequence-specific endonuclease gene editing techniques, such as the Cas9 nuclease from the microbial clustered regularly interspaced short palindromic repeats (CRISPR), allow researchers to introduce or knockout endogenous genomic segments in eukaryotes [54]. The CRIPSR Cas9 nuclease system works by having the nuclease Cas9 guided to the appropriate cleavage or insertion site by small RNAs, 20 nucleotides long, through Watson-Crick base pairing with the target DNA sequence [55]. This makes it easier to design and highly specific. The Cas9 endonuclease imposes its genome editing action by stimulating a double-stranded break at the target genomic locus. Once the double-stranded break has occurred the DNA segment follows one of two DNA damage repair pathways, the non-homologous end joining pathway (NHEJ) or the homology-directed repair pathway (HDR) [56, 57, 58, 59]. Which pathway is used for DNA repair relies on several factors, the key of which is whether a repair template is present, necessary for initiation of the HDR pathway [57]. The activation of a certain pathway can be used to the researcher's advantage. For example activation of the NHEJ pathway is especially useful in gene knockouts due to the formation of insertion/deletion mutations. The HDR pathway on the other

hand would be useful when precise, and defined modifications are necessary at a target locus, using an exogenously introduced repair template [54, 60].

When compared to other genome editing techniques such as zinc-finger nucleases (ZFNs) and transcription activator-like effector nucleases (TALENs), the Cas9 nuclease system offers several different advantages. It is easier to customize targets and action (insertion/deletion), simply by changing the 20 nucleotide sequence you can retarget the nuclease to a new DNA sequence. Although, the TALENs system can be re-edited to change DNA targets, it is more time intensive to construct new pairs of TALENs [61]. ZFNs are excessively difficult to engineer in compared to both the CRISPR system and the TALENs system [62, 63]. The CRISPR/Cas9 system also has a higher targeting efficiency and it can facilitate multiplex genome editing, making it an easy choice when considering gene editing [56].

One limitation however, to possible targeting sites is the fact that the presence of a protospacer adjacent motif (PAM) sequence is required directly 3' of the 20 base pair target sequence on the DNA. Ultimately this limitation only slightly decreases the number of possible targeting sequences since on average there is a PAM sequence present in the human genome every 8-12 base pairs [64].

Retroviruses and Lentiviral Delivery of Nucleic Acids

Over the last decade lentiviral delivery has emerged as leading delivery methods of nucleic acids to a variety of cell types, especially difficult-to-transfect cells, in a multitude of experimental

models. Lentiviruses are a part of the Retroviridae family, categorised due to their ability to retrotranscribe their RNA-based genome into linear double-stranded deoxyribonucleic acid, thereby allowing their genome to integrate into the host genome [65]. Categorization of the various subtypes of the Retroviridae family relies on the different accessory and regulatory genes present in complex or simple retroviruses. All retroviruses share a common structure which, starting from the outer-most layer, is comprised of the host cell membrane-derived envelope covered with envelope glycoprotein (ENV), then the outer layer of protein comprised of the matrix protein (MA), and finally the inner core containing two copies of single-stranded RNA, viral reverse transcriptase (RT), nucleocapsid (NC), capsid (CA), integrase (IN), protease (PR), amongst other enzymatic proteins [65].

The most well-studied and commonly used lentivirus in research is HIV-1. It has a 7-9kb genome containing the three major structural genes: Gag, Pol and Env [66]. Each gene plays a key role in the viral life-cycle. Once transcribed Gag is cleaved into three transcripts encoding three different viral core proteins, MA, CA, and NC [65, 66]. The MA proteins are essential for virion assembly and facilitate the infection of quiescent cells. The CA proteins form the core of the virion and finally the NC proteins shield the viral genome through tight associations with the viral RNA. The Pol gene is responsible for expressing the viral protease (PR), reverse transcriptase (RT) and integrase (IN) all of which are necessary for replication. The Env gene expresses surface glycoprotein gp160, which through cell receptor binding or fusion with the cellular membrane allow for viral entry into the host cell [65, 66]. Finally there are two long terminal repeat (LTR) promotor sequences flanking the viral genome which are necessary for proper viral transcription and reverse transcription and integration to occur.

While simple retroviruses encode the three main polyproteins, Gag, Pol and Env, complex retroviruses, such as lentivirus, can be distinguished based on the expression of six additional regulatory or accessory proteins, ultimately implicated in regulation of transcription, gene expression and viral particle assembly [65, 67]. These include the RNA-binding protein Rev, which is responsible for late-phase gene expression and the transport of structural protein encoding mRNAs, into the cytoplasm. Tat, another regulatory gene present in lentiviruses, responsible for enhancing transcription of the viral genome by encoding transactivators. The Nef protein, present in complex retroviruses, functions to inhibit T-cell activation and the Vpu protein works to enhance viral release from the cell's membrane into the cytoplasm upon initial infection [65, 68]. Finally the Vif protein expressed plays a key role in the replication cycle of the lentivirus by downregulating the host's antiviral immune responses.

Lentiviral Vectors

Ordinarily derived from the human immunodeficiency virus (HIV), lentiviral vectors can be used to deliver genomic segments of interest to virtually any mammalian target cell type. There are numerous advantages of using a lentiviral vector delivery system including their ability to mediate potent transduction in cell types otherwise considered difficult-to-transfect [68, 69]. This delivery method does not rely on the cell cycle for its action, unlike other many other retroviruses, since transduction and expression can be achieved in both dividing and quiescent cells. Lentiviral delivery is reliable in both in vitro and in vivo experiments effectively increasing research potential. Another advantage is the fact that lentiviral vectors are subject to Tet- or Cre-based regulation and integration of fluorescent reporters, allowing for tissue-specific expression and easy visualization [69, 70]. These advantages, plus it's entirely customizable nature from the

promotors chosen, to the reporters and tags utilized, makes lentiviral vectors the perfect vehicle for delivery of CRISPR gene knockout plasmids to target cells.

Second Generation vs. Third Generation Lentivirus

The second generation lentiviral system is comprised of three plasmids, each encoding different genes from the lentiviral genome, required for packaging, transfer and envelope generation. The packaging plasmid expresses the HIV derived Gag, Pol, Rev and Tat genes [69, 70]. The transfer plasmid encodes the long terminal repeat (LTR) promoter driving gene expression in a Tat-dependent fashion. The transfer plasmid also contains the gene of interest that is to be integrated into the host cell's genome. Finally the envelope plasmid contains the envelope protein Env, the most commonly used of which is the VSV-G due to its extensive range of infectivity for a multitude of cell types [71]. It is important to note that second generation lentiviral systems are reliant on Tat, an HIV protein, for viral expression and therefore can only be packaged by a second generation packaging system [70].

The third generation lentiviral system is generally considered safer than the second generation and consists of four plasmids [70]. There are two packaging plasmids, one encoding the Rev gene and the second encoding the Gag and Pol genes. Splitting the packaging system components is considered safer because it further reduces the chance occurrence of generation of replication-competent lentivirus [69, 70]. Additionally the third generation lentiviral system does not include Tat to generate virus, instead it utilizes a 5'LTR that is fused to heterologous promoter such as CMV or RSV. Third generation lentiviral systems can also include a self-inactivating vector. The self-inactivating vector includes a deletion in the 3'LTR which is

conveyed in the 5'LTR following the first cycle of reverse transcription, effectively eliminating the potential for production of a replication-competent lentivirus [69, 70].

LentiCRISPR Plasmids

Originating as a microbial nuclease defence system against invading plasmids and phages, CRISPR was transformed into a gene editing tool, utilized in research on a global scale [60]. The microbial CRISPR loci are made up of CRISPR-associated genes, termed Cas, and RNA segments that can be manipulated to achieve site specific CRISPR-mediated genomic cleavage [60]. LentiCRISPR plasmids combine the utility of that exact CRISPR/Cas system characteristic, to generate site specific cleavage, and the ability of the lentiviral system to deliver the CRISPR/Cas system into virtually any mammalian target cell [72].

There are several types of LentiCRISPR vectors available and determining the appropriate one for use depends upon the intended application. One example is the LentiCRIPSRv2 which is a singular vector system that contains two expression cassettes, a Cas9 nuclease encoded and a custom guide RNA [72, 73]. The guide RNA is a 20bp sequence that bind to a target region on the gene of interest and allows for highly specific genomic alteration. The annealed guide RNA is incorporated into the LentiCRISPRv2 vector at the BsmBl digestion site present on the vector. The vector also contains puromycin resistance genes allowing for reliable selection of transduced bacterial clones and later for assessment of transduction and expression efficiency in target cells [72, 73].

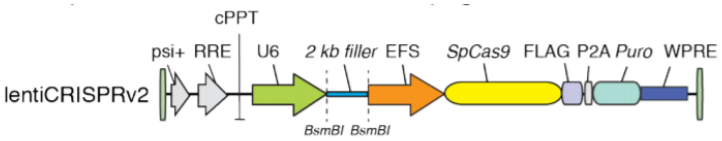

Supplementary Figure 1: LentiCRISPRv2 vector, illustrating the sequence components of the plasmid. U6 promotor for expression. SpCas9 nuclease for genomic cleavage. Puromycin resistance allowing for bacterial clone selection and affirmation of integration/expression of the plasmid.

LentiCRISPR delivery of genomic segments into bone marrow

LentiCRISPR delivery of genetic editing to bone marrow cells has been documented in multiple studies in the literature. In a study by Holmgaard et al (2017), investigators utilized LentiCRISPR, spCas9 and sgRNA, mediated genome editing and knockout to develop a novel treatment for acquired retinal diseases [74]. They developed three separate guide RNAs, incorporated into their respective LentiCRISPR vectors, each selective for their own target region on the vascular endothelial growth factor (*Vegfa)* gene and targeted for delivery via LentiCRISPR vectors to the retina. Results demonstrated that the LentiCRISPR system led to high frequencies of indel formation when tested both in vitro and in vivo in the target gene. That in turn led to a significant reduction in the incidence of a number of ocular diseases tested, including age-related macular degradation, when explored in appropriate murine ocular disease models [74]. In another study by Wang et al (2015), the LentiCRISPR gene editing system was successfully utilized for in situ gene transfer into hematopoietic stem cells of a murine experimental model [75]. In this study the researchers transferred a factor VIII (FVIII) transgene or green fluorescence protein into bone marrow cells, in vivo in an animal model, in order to

investigate the application potential of lentiviral delivery systems for genetic modification and implications for treatment of FVIII deficiencies. They concluded that the delivery method was a viable option for in vivo gene transfer and a potentially novel treatment for FVIII gene deficiencies, such as hemophilia A [75].

2.0 Methods and Results:

Hematopoietic Stem Cells are a Promising Target for Genetic Modification of C5

Data from expression libraries was analyzed by Dr. Anna Dvorkin, McMaster University, Hamilton, to determine which cell types produce complement component C5 both in humans, where gene is termed C5, and in mice, where the gene is termed hemolytic complement (Hc). Results generated support that there are multiple types of cells that express complement component C5 and the majority of those cell types are of hematopoietic stem cell origin (Figures 1&2). This in turn supports targeting of hematopoietic stem cells (CD34+) for genetic modification as a means to reduce donor derived complement C5 levels.

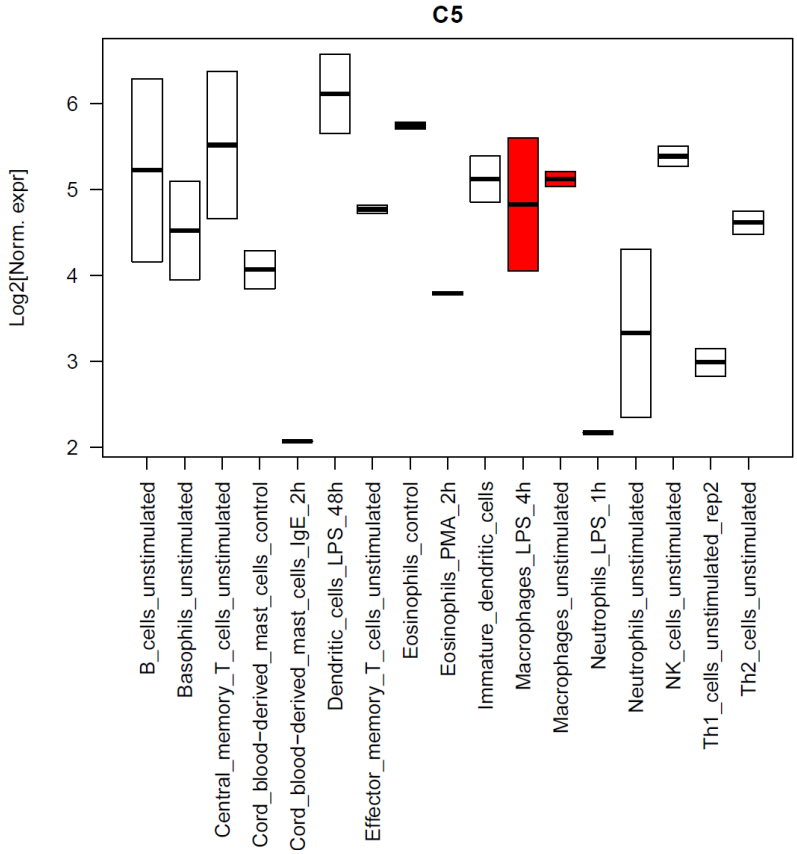

Figure 1: Boxplots showing levels of normalized expression for C5 across different cell types obtained from mouse. Publicly available data was obtained from GSE3982 (Affymetrix HG-U133A microarray). Each group had n = 2. Macrophages marked in red.

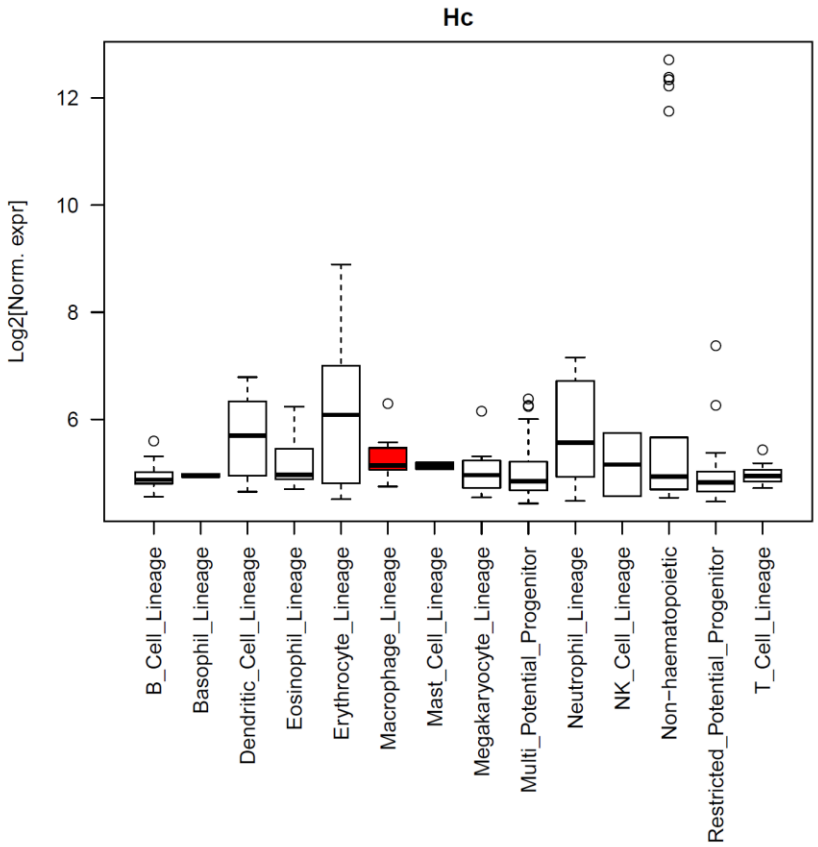

Figure 2: Boxplots showing levels of normalized expression for Hc across different cell types obtained from mouse. Publicly available data was obtained from GSE77098 (Illumina MouseWG-6 microarray). N = 2-7 per group. Macrophages marked in red.

Design of Complement Component C5 Specific CRISPR/Cas9 Knockout Plasmid

In order to assess the role complement component C5 plays in the initiation of GvHD a pCas-Guide-EF1a-GFP, 10kb, plasmid was purchased from OriGene (Cat# GE200649). The plasmid contains a U6 promoter, to enable transcription of the plasmid in the target cells and 20bp guide RNA sequence specific for a target region on the murine complement component C5 gene (Table 1). It also encodes for a Cas9 nuclease that is guided to the target cleavage site by the guide RNA sequence. A GFP marker is encoded by the plasmid for easy visualization of transfection efficiency and expression of the plasmid in target cells, in this case murine BM cells.

Table 1: CRISPR/Cas9 sgRNA Sequence

sgRNA	sgRNA sequence
sgRNA	GATACTCTACCTGACTGGTC

Table 1: sgRNA sequence targeting specific region in the murine C5 gene. Sequence was incorporated into a CRISPR/Cas9 plasmid.

Lipofectamine Produces High Transfection Rate in HEK 293T with CRISPR/Cas9 Knockout Plasmid

To verify that the plasmid was an appropriate size for transfection into mammalian cells and to assess the U6 promoter function, HEK 293T cells were transfected using lipofectamine 2000 (ThermoFisher Cat# 11668030). Four lipofectamine concentrations were tested; 6µL, 9µL, 12µL, 15µL. Each of the four lipofectamine conditions were added to HEK 293T cells at 70% confluence in a petri dish and incubated overnight in a 37 degree Celsius, 5% CO_2 in air incubator. Cells were then viewed under an EVOS fluorescence microscope imagining system at 40x magnification to determine transfection efficiency. Five images were captured from each condition and the experiment was repeated five times to demonstrate reproducibility of results. Transfection averages were calculated for each condition based on all images taken for that condition in all five repetitions of the experiment (Table 2). As can be seen in Table 2 the condition that showed the highest transfection rates in HEK 293T cells was 12 µL with approximately 85% transfection.

Table 2: Transfections of HEK 293T Cells with CRISPR/Cas9 Plasmid via Lipofectamine

Lipofectamine Added	BM Cell Count	% GFP
6 µL	$1x10^6$	70
9 µL	$1x10^6$	70

12 µL	$1x10^6$	85
15 µL	$1x10^6$	80

Table 2: Transfection efficiency is determine as number of GFP positive cells out of total number of cells on the image captured. Five images were captured from each condition and transfection averages (%GFP) were calculated and represented.

Nucleofection of Murine Bone Marrow with CRISPR/Cas9 Plasmid Results in Low Transfection Rate

Nucleofection was tested as a means to transfect murine bone marrow cells with the CRISPR/Cas9 plasmid. Three different nucleofection kits were tested, Human CD34+ Cell kit (Cat# VPA-1003), Mouse Embryonic Stem Cell kit (Cat# VPH-1001) and a Human Mesenchymal Stem Cell kit (Cat# VVPE-1001). Bone marrow cells were centrifuged at 161 RCF for 10 minutes and supernatant was discarded. Cell pellet was resuspended in 100µl of optimem media. 4µg of plasmid was added to the cell suspension. Suspension was then transferred to a 2mm electroporation cuvette that came with the nucleofection kit and the cuvette was places in Nucleofector 2b device (from Lonza). Various nucleofection programs, with increasing intensity, were tested. Following nucleofection the cells were removed from the cuvette using a thin tipped pipette and transferred to a well of a six well plate containing 2ml of warmed media. The plate was then transferred to incubate for 24 hours in a 37 degrees Celsius, 5% CO_2 in air incubator. Following the incubation cells were visualized under the EVOS fluorescence microscope imagining system to detect the percent of GFP expressing cells as a

means to determine transfection efficiency (Tables 3-6). The highest transfection rate observed was 10% using the Human CD34+ Cell kit and the V-029 program on the Nucleofector 2b device, 24 hours post-nucleofection (Table 4).

Table 3: Optimization of nucleofection for resting murine BM cells with Human CD34+ kit

Settings	%GFP of experimental plasmid	Viability (%)	Control Plasmid GFP (%)	Viability (%)
U-008	0	80	0	87
U-009	0	72	0	81
U-010	0	75	0	77
U-011	0	67	0	74
U-012	0	77	0	71
U-013	0	68	0	62
U-014	0	62	0	64
U-015	0	74	0	58
U-016	0	67	0	63
U-017	0	68	0	72
U-018	0	70	0	73
U-019	0	69	0	61
U-020	0	66	5	59

GFP expression of murine bone marrow cells and cell viability (%) were measured 24 hours post-nucleofection using Nucleofector 2b programs of increasing intensity, starting at U-008 until U-020.

Table 4: Optimization of nucleofection for resting murine BM cells with Human CD34+ kit

Settings	%GFP of experimental plasmid	Viability (%)	Control Plasmid GFP (%)	Viability (%)
U-021	5	67	20	66
U-023	5	71	26	63
U-028	0	65	0	62
U-030	0	60	0	62
U-033	0	51	15	57
V-024	0	58	0	44
V-028	0	46	0	41
V-029	10	42	15	40

GFP expression of murine bone marrow cells and cell viability (%) were measured 24 hours post-nucleofection using Nucleofector 2b programs of increasing intensity, starting at U-021 until U-029.

Table 5: Optimization of nucleofection for resting murine BM cells with Mouse Embryonic Stem Cell kit

Settings	%GFP of experimental plasmid	Viability (%)	Control Plasmid GFP (%)	Viability (%)
U-021	0	84	0	78
U-023	0	84	0	81
U-028	0	79	0	76
U-030	0	61	0	76
U-033	0	63	0	70

V-024	0	56	0	54
V-028	0	55	0	54
V-029	0	32	0	47

GFP expression of murine bone marrow cells and cell viability (%) were measured 24 hours post-nucleofection using Nucleofector 2b programs of increasing intensity, starting at U-021 until U-029.

Table 6: Optimization of nucleofection for resting BM cells with Human Mesenchymal Stem Cell kit

Settings	%GFP of experimental plasmid	Viability (%)	Control Plasmid GFP (%)	Viability (%)
U-021	0	63	0	70
U-023	0	63	0	71
U-028	0	56	0	66
U-030	0	57	0	62
U-033	0	49	0	63
V-024	0	31	0	54
V-028	0	33	0	55
V-029	0	30	5	46

GFP expression of murine bone marrow cells and cell viability (%) were measured 24 hours post-nucleofection using Nucleofector 2b programs of increasing intensity, starting at U-021 until U-029.

Electroporation of Murine Bone Marrow with CRISPR/Cas9 Plasmid Results in Low Transfection Rate

In order to transfect murine bone marrow cells with the CRISPR/Cas9 plasmid electroporation was used. Bone marrow cells were centrifuged at 161 RCF for 10 minutes and supernatant was discarded. Cell pellet was resuspended in 10ml of opti-MEM media (ThermoFisher, Cat# 31985070). This washing was repeated 3 times with opti-MEM media. Cells were then resuspended to a volume of 100μl and 5μg of plasmid was added to the cell suspension. Suspension was then transferred to a 2mm electroporation cuvette (BTX, Model# 620) and the cuvette was places in ECM 830 square wave electroporator (from BTX). Following electroporation the cells were removed from the cuvette using a thin tipped pipette and transferred to a well of a six well plate containing 2ml of warmed media. The plate was then transferred to incubate for 24 hours in a 37 degrees Celsius, 5% CO_2 in air incubator. Following the incubation cells were visualized under the EVOS fluorescence microscope imagining system to detect of percent GFP expressing cells as a means to determine transfection efficiency (Table 7). Cells were then returned to the incubator for another 24 hours. Following the 48 hour total incubation transfection efficiency was again determined (Table 8). Highest transfection efficiencies detected were 5% using the 460V/0.2ms, the 500V/0.5ms and 360V/5ms condition 48 hours post-electroporation (Table 8).

Table 7: Optimization of electroporation for resting murine bone marrow cells

Settings	%GFP	Viability (%)
200 V/50 ms	0	76
200 V/20 ms	0	70
300 V/10 ms	N/A	N/A
300 V/5 ms	0	72
360 V/5 ms	0	54
360 V/2 ms	0	60
360 V/1 ms	0	60
400 V/0.5 ms	0	38
460 V/0.2 ms	0	41
500V/0.5ms	0	30

GFP expression of murine bone marrow cells and cell viability (%) were measured 24 hours post-electroporation

Table 8: Optimization of electroporation for resting murine bone marrow cells

Settings	%GFP	Viability (%)
200 V/50 ms	0	74
200 V/20 ms	0	70
300 V/10 ms	N/A	N/A
300 V/5 ms	0	68
360 V/5 ms	5	47
360 V/2 ms	3	55
360 V/1 ms	0	60
400 V/0.5 ms	0	31
460 V/0.2 ms	5	40
500V/0.5ms	5	29

GFP expression of murine bone marrow cells and cell viability (%) were measured 48 hours post-electroporation.

Polymer Delivery of CRISPR/Cas9 Knockout Plasmid Results in Low Transfection Rate

In order to deliver the CRISPR/Cas9 knockout plasmid into murine bone marrow cells five cationic polymer polyelectrolyte complexes were provided by Dr. Ali Akbari in Dr. Hoare's lab, McMaster University, Hamilton and tested by Ekaterina Todorova. The first polymers were Chitosan: Tripolyphosphate (Chitosan:TPP) based, Figure 3, and a two different ratios, the first at Chitosan:TPP 5/1.25 mg/mL at pH 6.5 (590 nm and +15 mV) and the second at Chitosan:TPP 2.5/0.6 mg/mL at pH 6.5 (208 nm and +8 mV). Chitosan was chose for its positive charge, allowing for electrostatic interactions with the negatively charged CRISPR/Cas9 plasmid. The third polymer tested was O-carboxymethyl chitosan: Tripolyphosphate (CMCS:TPP), Figure 4 at pH 7 (225 nm and -10 mV). This polymer was chosen due to the amine group present that would allow it to bind to the plasmid more effectively and presence of the carboxyl group in CMCS structure which could potentially improve plasmid release following cellular uptake. The final two polymers tested were poly-oligoethyleneglycol monomethyl ether methacrylate: N,N-dimethylaminoethyl methacrylate (POEGMA:DMAEMA), Figure 5, based at two different ratios. The first was POEGMA:DMAEMA 10:90% at pH 9 (+3 mV and 320 nm) and the second was POEGMA:DMAEMA 25:75% at pH 9 (+3 mV and 480 nm). This polymer was chosen because the DMAEMA, with a pKa of 8.4 in complex with POEGMA at different ratios may potentially show different plasmid bonding and release behaviors. Polymers were added to either $1x10^6$ or $2x10^6$ BM cells in a six well plate and incubated for 24 hours in a 37 degrees Celsius, 5% CO_2 incubator. Following the incubation cells were visualized under the EVOS fluorescence microscope imagining system to detect of percent GFP expressing cells as a means to determine transfection efficiency (Tables 9-11). Cells were then returned to the incubator for another 24

hours. Following the 48 hour total incubation transfection efficiency was again determined. Chitosan:TPP 2.5/0.6 mg/ml and 4µg produced the highest transfection rate of 5% (Table 10). Figures 6-10 illustrate representative images from the different polymer based transfections.

Figure 3: Chitosan:TPP polymer tested

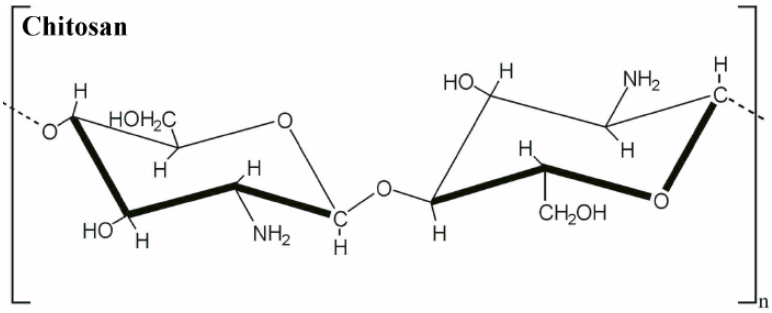

Figure 3: Depicting the chitosan as part of the polymer complex chitosan:TPP, at pH 6.5 (590 nm and +15 mV), utilized in polymer based transfections of murine BM cells with CRISPR/Cas9 plasmid.

Figure 4: CMCS:TPP polymer tested

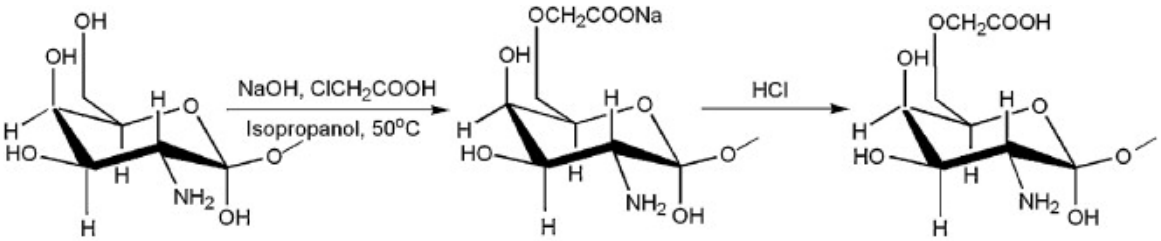

Figure 4: Demonstrates the CMCS:TPP polymer at pH 7 (225 nm and -10 mV) tested. Amine group that would bind plasmid is shown as well as the carboxyl group in CMCS, which could aim in improving plasmid release following cellular uptake.

Figure 5: Components of POEGMA:DMAEMA polymer tested

POEGMA

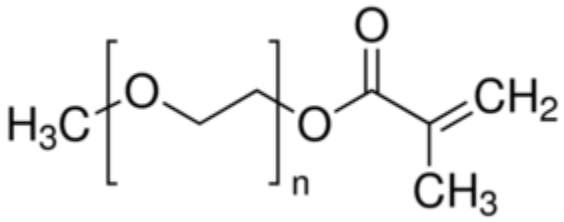

DMAEMA

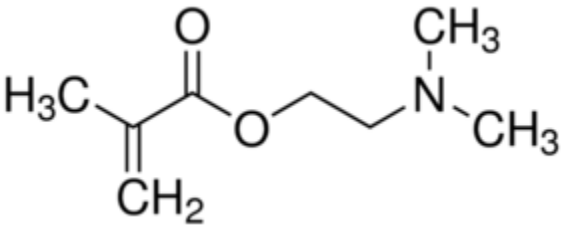

Figure 5: Illustrates the structures of the two components that make up the POEGMA:DMAEMA polymer, at pH 8.5 (+5 mV and 480 nm), tested.

Table 9: CRISPR/Cas9 Plasmid Transfection of Murine BM via Polymer Delivery

Polymer Complex	[Plasmid]	BMCell Quantity	GFP (%)
Chitosan: TPP 2.5/0.6 mg/mL	2µg	$1x10^6$	1
Chitosan: TPP 2.5/0.6 mg/mL	2µg	$2x10^6$	1
Chitosan: TPP 2.5/0.6 mg/mL	4µg	$1x10^6$	4
Chitosan: TPP 2.5/0.6 mg/mL	4µg	$2x10^6$	4
Chitosan: TPP 5/1.25 mg/mL	2µg	$1x10^6$	1
Chitosan: TPP 5/1.25 mg/mL	2µg	$2x10^6$	1
Chitosan: TPP 5/1.25 mg/mL	4µg	$1x10^6$	2
Chitosan: TPP 5/1.25 mg/mL	4µg	$2x10^6$	2
POEGMA:DMAEMA 10%: 90%	2µg	$1x10^6$	0
POEGMA:DMAEMA 10%: 90%	2µg	$2x10^6$	0
POEGMA:DMAEMA 10%: 90%	4µg	$1x10^6$	1
POEGMA:DMAEMA 10%: 90%	4µg	$2x10^6$	1
POEGMA:DMAEMA 25%: 75%	2µg	$1x10^6$	0
POEGMA:DMAEMA 25%: 75%	2µg	$2x10^6$	0
POEGMA:DMAEMA 25%: 75%	4µg	$1x10^6$	1
POEGMA:DMAEMA 25%: 75%	4µg	$2x10^6$	1
Control: H_2O + Plasmid DNA	2µg	$1x10^6$	0
Control: H_2O + Plasmid DNA	2µg	$2x10^6$	0
Control: H_2O + Plasmid DNA	4µg	$1x10^6$	1
Control: H_2O + Plasmid DNA	4µg	$2x10^6$	1

Table 9: 24 hours post-transfection of either $1x10^6$ or $2x10^6$ BM cells via Chitosan: TPP 2.5/0.6 mg/mL, Chitosan: TPP 5/1.25 mg/mL, POEGMA:DMAEMA 10:90%, POEGMA:DMAEMA 25:75% or Control of H2O and plasmid DNA. %GFP represents the transfection rate.

Table 10: CRISPR/Cas9 Plasmid Transfection of Murine BM via Polymer Delivery

Polymer Complex	[Plasmid]	Cell Quantity	GFP (%)
Chitosan: TPP 2.5/0.6 mg/mL	2µg	$1x10^6$	1
Chitosan: TPP 2.5/0.6 mg/mL	2µg	$2x10^6$	1
Chitosan: TPP 2.5/0.6 mg/mL	4µg	$1x10^6$	5
Chitosan: TPP 2.5/0.6 mg/mL	4µg	$2x10^6$	5
Chitosan: TPP 5/1.25 mg/mL	2µg	$1x10^6$	1
Chitosan: TPP 5/1.25 mg/mL	2µg	$2x10^6$	1
Chitosan: TPP 5/1.25 mg/mL	4µg	$1x10^6$	2
Chitosan: TPP 5/1.25 mg/mL	4µg	$2x10^6$	2
POEGMA:DMAEMA 10%: 90%	2µg	$1x10^6$	0
POEGMA:DMAEMA 10%: 90%	2µg	$2x10^6$	0
POEGMA:DMAEMA 10%: 90%	4µg	$1x10^6$	1
POEGMA:DMAEMA 10%: 90%	4µg	$2x10^6$	1
POEGMA:DMAEMA 25%: 75%	2µg	$1x10^6$	0
POEGMA:DMAEMA 25%: 75%	2µg	$2x10^6$	0
POEGMA:DMAEMA 25%: 75%	4µg	$1x10^6$	1
POEGMA:DMAEMA 25%: 75%	4µg	$2x10^6$	1
Control: H_2O + Plasmid DNA	2µg	$1x10^6$	0
Control: H_2O + Plasmid DNA	2µg	$2x10^6$	0
Control: H_2O + Plasmid DNA	4µg	$1x10^6$	1
Control: H_2O + Plasmid DNA	4µg	$2x10^6$	1

Table 10: 48 hours post-transfection of either $1x10^6$ or $2x10^6$ BM cells via Chitosan: TPP 2.5/0.6 mg/mL, Chitosan: TPP 5/1.25 mg/mL, POEGMA:DMAEMA 10:90%, POEGMA:DMAEMA 25:75% or Control of H2O and plasmid DNA. %GFP represents the transfection rate.

Table 11: CRISPR/Cas9 Plasmid Transfection of Murine BM via Polymer Delivery

Polymer Complex	[Plasmid]	BMCell Quantity	GFP (%)
CMCS: TPP 2.5/0.6 mg/mL	2µg	$1x10^6$	3
CMCS: TPP 2.5/0.6 mg/mL	2µg	$2x10^6$	3
CMCS: TPP 2.5/0.6 mg/mL	4µg	$1x10^6$	5
CMCS: TPP 2.5/0.6 mg/mL	4µg	$2x10^6$	4
Control: H_2O + Plasmid DNA	2µg	$1x10^6$	0
Control: H_2O + Plasmid DNA	2µg	$2x10^6$	0
Control: H_2O + Plasmid DNA	4µg	$1x10^6$	1
Control: H_2O + Plasmid DNA	4µg	$2x10^6$	0

Table 11: 24 hours post-transfection of either $1x10^6$ or $2x10^6$ BM cells via CMCS:TPP or Control of H2O and plasmid DNA. %GFP represents the transfection rate.

Figure 6: BM cell transfection with CRISPR/Cas9 plasmid via Chitosan:TPP 5/1.25 mg/ml

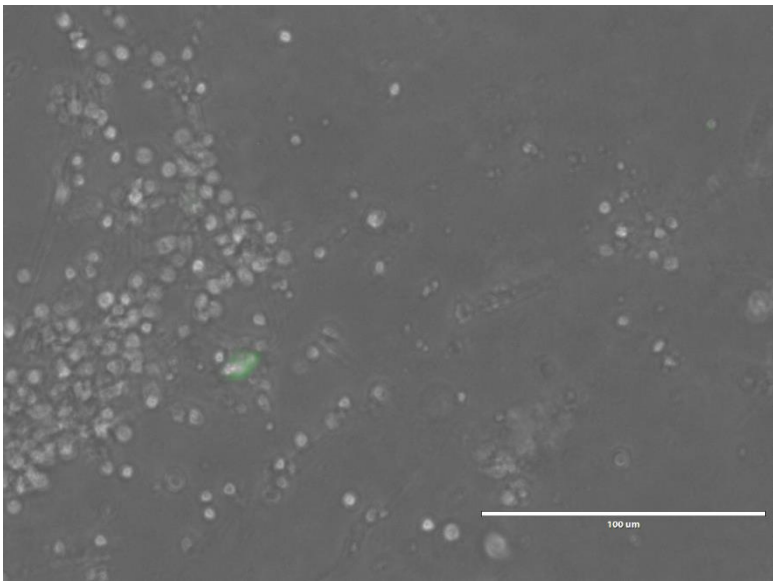

Figure 6: Representative image of 24 hours post-transfection of 2x10 BM cells with CRISPR/Cas9 plasmid via Chitosan:TPP 5/1.25 mg/ml carrying 4ug of plasmid DNA delivery. Chitosan:TPP 5/1.25 mg/mL is at a pH 6.5 and 590 nm and +15 mV respectively. Demonstrates a transfection rate of approximately 2%.

Figure 7: BM cell transfection with CRISPR/Cas9 plasmid via Chitosan:TPP 2.5/0.6 mg/ml

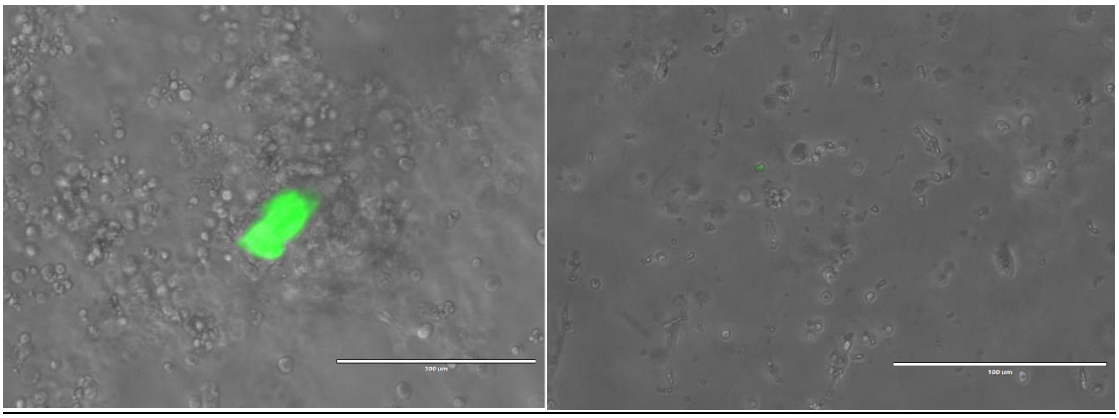

Figure 7: Representative images of 24 hours post-transfection of 2x10 BM cells with CRISPR/Cas9 plasmid via Chitosan:TPP 2.5/0.6 mg/ml carrying 4ug of plasmid DNA delivery. Chitosan:TPP 2.5/0.6 mg/ml is at a pH of 6.5 and 208 nm and +8 mV respectively. Demonstrates a transfection rate of approximately 4%.

Figure 8: BM cell transfection with CRISPR/Cas9 plasmid via Control (H2O + Plasmid)

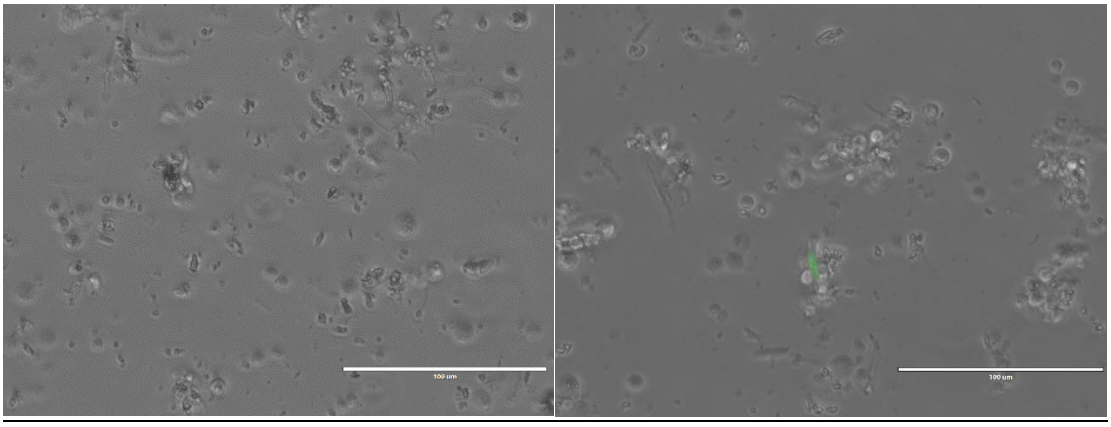

Figure 8: Representative images of 24 hours post-transfection of 2x10 BM cells with CRISPR/Cas9 plasmid via Control (H2O and 4ug of plasmid DNA). Demonstrates a transfection rate between 0-1%.

Figure 9: BM cell transfection with CRISPR/Cas9 via POEGMA:DMAEMA 10:90%

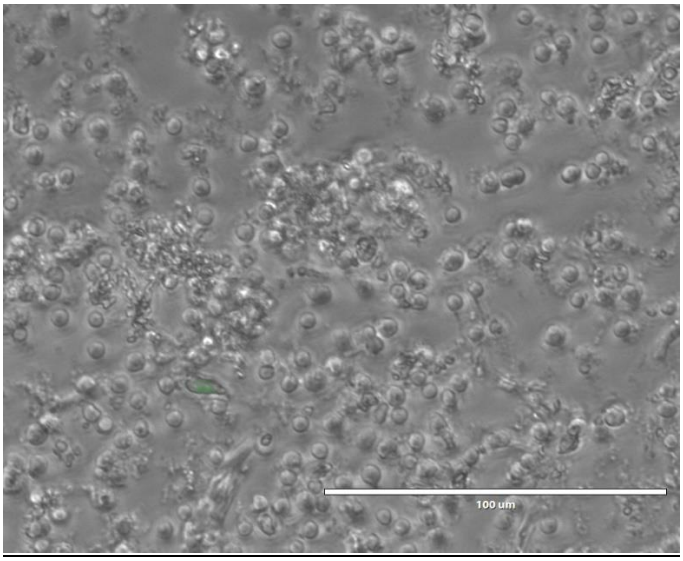

Figure 9: Representative images of 24 hours post-transfection of 2x10 BM cells with CRISPR/Cas9 plasmid via POEGMA:DMAEMA 10:90% at a pH of 9 and+3 mV and 320 nm respectively, carrying 4ug of plasmid DNA. Demonstrates a transfection rate of approximately 1%.

Figure 10: BM cell transfection with CRISPR/Cas9 via POEGMA:DMAEMA 25:75%

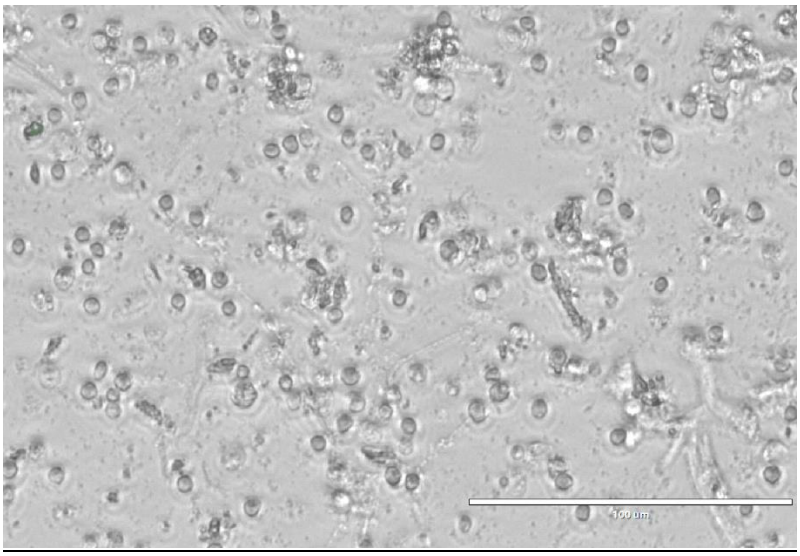

Figure 10: Representative images of 24 hours post-transfection of 2x10 BM cells with CRISPR/Cas9 plasmid via POEGMA:DMAEMA 25:75% at a pH of 9 and+3 mV and 480 nm respectively, carrying 4ug of plasmid DNA. Demonstrates a transfection rate of approximately 1%.

GvHD is developed following an allogeneic-whole bone marrow transplant in murine model

Murine Model of GvHD

To be able to further understand and study the role of C5 in GvHD, in vivo, we recreated a murine model of the disease state. Six to eight week-old female complement component C5 competent (Qa2$^-$ BALB/cByJ from Jackson Laboratory) recipient mice were irradiated with 650 RADs. Recipient mice were left to rest and recover in ventilated cages on a heating pad. The recipient mice in this experiment were termed the Trial group. Spleen and bone marrow cells were then harvested from C5 competent donor mice (B10.D2-Hc^1 H2^d H2-T18^c /nSnJ Jackson Laboratory). Bone marrow cells were harvested from the femur and tibias of donor mice via grinding with a mortar and pestle in phosphate-buffered saline (PBS) and then filtered through a 70μm cell strainer. Spleen cells were harvested from the donor spleen by rupturing the spleen with a 1mL syring in a petri dish containing 5mL of PBS. Spleen suspension was then filtered through a 40μm strainer. Both spleen and bone marrow cells were processed using Ammonium-Chloride-Potassium (ACK) lysis buffer to lyse and remove red blood cells (RBC) and washed twice with 10mL PBS. Spleen and bone marrow cells were then counted using the countess automated cell counter and resuspended in 200μl of PBS. Six hours following the sub-lethal irradiation recipient mice were transplanted, under isofurane gaseous anesthesia, via retro-orbital (RO) injection with $2x10^6$ spleen cells and either $1x10^6$ or $2x10^6$ bone marrow (BM) cells previous harvested from donor mice. Mice were then maintained in an ultraclean level 2 housing for the first two weeks following the transplant and then transferred to clean vent housing for the remaining six weeks. Mice were harvested via euthanasia on day 60 post-transplant to determine whether development of GvHD occurred. To achieve this airway physiology was evaluated using

FlexiVent automatic ventilator and then compared to two historical age-matched control groups previously performed by Dr. Jewel Imani, McMaster University, Hamilton [76]. These two groups were termed the Saline group and the C5 Deficient group. Mice in the saline group received a retro-orbital injection of 100µl of PBS. The same procedures were followed when transplanting the C5 deficient group, as were outlined above for the trial group, however mice in the C5 deficient group received bone marrow and spleen cells from C5 deficient donor mice (B10.D2-Hc^0 $H2^d$ H2-$T18^c$/oSnJ Jackson Laboratory). Housing conditions were the same for all mice included in this study, all groups were housed in the same facility and received the same diet and care.

There was no statistically significant difference in total airway resistance levels between historic C5 competent mice and current C5 competent mice termed control mice in this study

To validate the use of historical data from the Saline and C5 deficient mouse groups produced by Dr. Jewel Imani, Dr. Imani's C5 competent group, conducted at the same time as the other's, was compared to our control group. This comparison was possible because both the historic C5 competent group and the current control group were treated using the same protocol, mice were the same age, were house in the same facility and received the same diet and care. The difference between the Dr. Imani's C5 competent group and our control group was the time at which the experiment was performed. There was no significant difference in total airway resistance levels found between the C5 competent (C5+) historic group and the control group ($p = 0.089$) although visually a trend can be seen with the control group having higher total airway resistance than the historic C5+ group (Figure 11 and Table 12).

Ranks

	Group	N	Mean Rank	Sum of Ranks
TotalAirwayResistance	Controls	4	13.50	54.00
	C5+	15	8.36	117.00
	Total	19		

Test Statisticsb

	TotalAirwayResistance
Mann-Whitney U	12.000
Wilcoxon W	117.000
Z	-1.699
Asymp. Sig. (2-tailed)	.089
Exact Sig. [2*(1-tailed Sig.)]	.101

Table 12: Mann-Whitney test for total airway resistance between Dr. Imani's historical C5 competent group (labeled as C5+) and control group shows no statistically significant difference between the groups (p = 0.089).

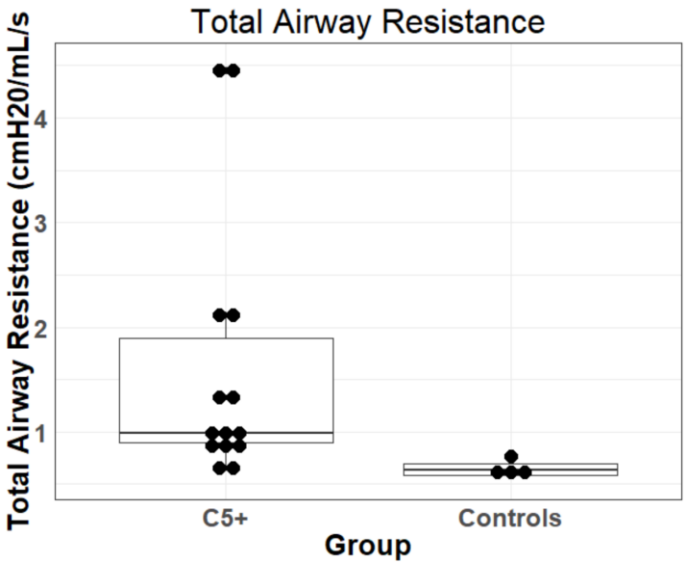

Figure 11: Mice transplanted by Dr. Jewel Imani with C5 competent donor bone marrow (termed C5+) has statistically similar levels of total airway resistance as the control group (p = 0.089). Sub-lethally irradiated BALB/c ($Qa2^-$) mice were transplanted with $2x10^6$ spleen cells and $2x10^6$ bone marrow cells from C5 competent donors. On day 60 post-transplant, a mechanical ventilator was used to measure total airway resistance. Data represents 2 independent experiments, results from which were pooled for each respective treatment group. C5+ group (n=5, 10) and control group (n=2, 2). C5+ group Q1=0.897, Q3=1.894, IQR=0.997, Median =0.988, Mean=1.621. Control group Q1=0.589, Q3=0.700, IQR=0.111, Median=0.640. Data was analyzed using a Mann-Whitney test to compare the two groups; °outliers of ±1.5 IQR from the median, one outlier was removed from control group, *P≤0.05.

There was no statistically significant difference in post-transplant survival rates between mice that received $1x10^6$ or $2x10^6$ BM cells in GvHD Murine Model

In order to assess the potential effect at two different concentrations, $1x10^6$ or $2x10^6$, bone marrow cells may have on the GvHD mouse model the experimental conditions were repeated with the higher concentration of BM cells. Two million spleen and $2x10^6$ bone marrow cells were transplanted into recipients to assess whether survival rates could be improved. The results showed no significant different in survival rate between mice in the $1x10^6$ or $2x10^6$ BM cell recipient group post-transplant (p = 0.483). (Table 13)

Group * Alive Crosstabulation

Count

		Alive		
		dead	alive	Total
Group	1 million BM cells	5	15	20
	2 million BM cells	6	10	16
Total		11	25	36

Chi-Square Tests

	Value	df	Asymp. Sig. (2-sided)	Exact Sig. (2-sided)	Exact Sig. (1-sided)
Pearson Chi-Square	.655	1	.418		
Continuity Correctionb	.198	1	.656		
Likelihood Ratio	.652	1	.419		
Fisher's Exact Test				.483	.327
Linear-by-Linear Association	.636	1	.425		
N of Valid Cases	36				

Table 13: Chi-Square test for survival rates of recipients of 1 million (n=20) vs 2 million (n=16) bone marrow cells demonstrate no statistically significant difference between the groups (p = 0.483).

There was no statistically significant difference in total airway resistance or lung compliance between mice that received $1x10^6$ or $2x10^6$ BM cells in GvHD Murine Model

Total airway resistance measurements, taken using a mechanical rodent ventilator, were compared between recipient mice that had received $1x10^6$ or $2x10^6$ bone marrow cells to assess potential differences between the two conditions on the GvHD mouse model. The results showed no significant different in total airway resistance between mice in the $1x10^6$ and $2x10^6$ BM cell recipient groups 60 days post-transplant (p = 0.242) (Table 14). The same comparison was done for lung compliance levels and no significant difference was found between mice that had received $1x10^6$ BM cells and those that received $2x10^6$ BM cells in the GvHD mouse model (p = 0.101) (Table 15).

Ranks

	BM_Cells	N	Mean Rank	Sum of Ranks
TotalAirwayResistance	1 million BM cells	15	13.93	195.00
	2 million BM cells	10	10.50	105.00
	Total	25		

Test Statisticsb

	TotalAirwayResistance
Mann-Whitney U	50.000
Wilcoxon W	105.000
Z	-1.171
Asymp. Sig. (2-tailed)	.242
Exact Sig. [2*(1-tailed Sig.)]	.259

Table 14: Mann-Whitney test for total airway resistance of recipients of 1 million (n=15) vs 2 million (n=10) bone marrow cells demonstrate no statistically significant difference between the groups (p = 0.242).

Ranks

	BM Cells	N	Mean Rank	Sum of Ranks
Compliance	1 million BM cells	15	10.50	147.00
	2 million BM cells	10	15.30	153.00
	Total	25		

Test Statisticsb

	Compliance
Mann-Whitney U	42.000
Wilcoxon W	147.000
Z	-1.640
Asymp. Sig. (2-tailed)	.101
Exact Sig. [2*(1-tailed Sig.)]	.108

Table 15: Mann-Whitney test for lung compliance of recipients of 1 million (n=15) vs 2 million (n=10) bone marrow cells demonstrates no statistically significant difference between the groups ($p = 0.101$).

There Was No Observable Difference in Post-Transplant Body Condition Between Mice That Received $1x10^6$ or $2x10^6$ BM cells in GvHD Murine Model

To further assess the potential effect two different concentrations, $1x10^6$ or $2x10^6$, bone marrow cells may have on the GvHD mouse model post-transplant body conditions were evaluated. Mice had either received $1x10^6$ or $2x10^6$ bone marrow cells during transplantation. The results showed no visual difference in body condition between mice in the $1x10^6$ or $2x10^6$ BM cell recipient group post-transplant (Figure 12).

Figure 12: Body condition of recipient mice of 1 million (n=15) vs 2 million (n=10) bone marrow cells demonstrates no observable difference between the groups.

Rodent Mechanical Ventilator Assessed Lung Airway Physiology Suggests Development of GvHD in Murine Model

To quantifiably determine development of GvHD in this murine model recipient mice were harvested on day 60 post-bone marrow transplant using intraperitoneal injection of 10 mg/kg xylazine hydrochloride for sedation and subsequent intraperitoneal injection of 30mg/kg sodium pentobarbital for achieve appropriate level of sedation. Once at surgical plane a tracheotomy was performed on the mice and a 19-gauge cannula was inserted into the trachea. Using the cannula mice were attached to a rodent mechanical ventilator (Flexivent, SCIREQ) and 20mg/kg of rocuronium was administered via intraperitoneal injection in order to paralyze respiratory muscles and eliminate spontaneous breathing. The Flexivent ventilator supplied forced waveform oscillation to the mouse's lungs with ventilation of 10ml/kg of air at 150 breaths per minute. Flow, volume and airway pressure was recorded and the data was used to measure total airway resistance (R), conducting airway resistance (Rn), tissue resistance (G) and tissue elastance (H). The Salazar-Knowles equation was used to determine quasi-static

compliance (CST). Kruskal-Wallis test performed to compare the total airway resistance of the saline, C5 deficient and trial treatment groups and it demonstrated a statistically significant difference of $p = 0.001$ (Table 16). Subsequently a Mann-Whitney test was run between each group. A statistically significant difference of $p = 0.02$ was noted between the trial and C5 deficient treatment groups, with the trial group showing significantly higher total airway resistance (Figure 13 & Table 17). Comparison between the saline treated and trial groups also demonstrated a statistically significant different with $p = 0.002$, with the trial group having higher total airway resistance (Figure 13 & Table 18).

When comparing lung compliance between the saline treated, C5 deficient and trial groups a statistically significance difference is seen using the Kruskal-Wallis test ($p = 0.000$) (Table 19). The Mann-Whitney test for compliance data of the saline treated and trial groups shows a significance of $p = 0.002$ with the trial group having lower lung compliance (Figure 14 & Table 20). A subsequent Mann-Whitney test for compliance data between the C5 deficient and trial groups shows a significance of $p = 0.002$ with the trial group having lower lung compliance (Figure 14 & Table 21).

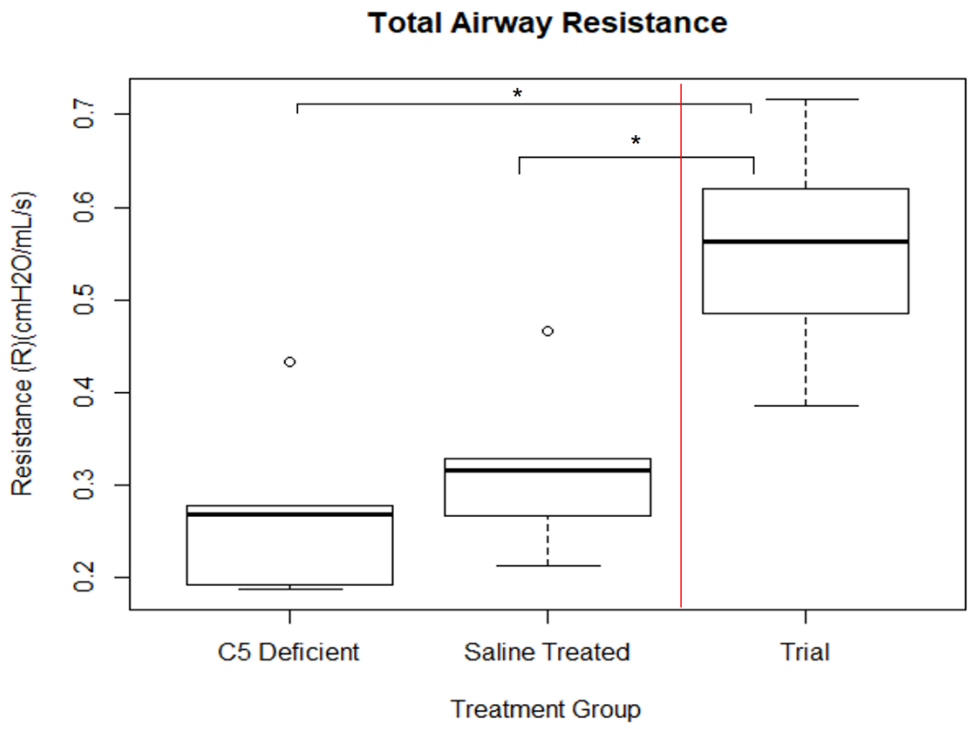

Figure 13: Mice transplanted with C5 competent donor bone marrow (termed trial mice) demonstrate an increased total airway resistance when compared to historical C5 deficient donor bone marrow recipient mice (p = 0.02) and saline treated mice (p = 0.02). Sub-lethally irradiated BALB/c(Qa2$^-$) mice were transplanted with 2x10^6 spleen cells and 2x10^6 bone marrow cells from C5 competent or C5 deficient donors or saline. On day 60 post-transplant, a mechanical ventilator was used to measure total airway resistance. Data represents 1-5 independent experiments, results from which were pooled for each respective treatment group. Trial group (n=3, 2, 1, 3, 3), C5 deficient transplant group (n=5), and saline group (n=5). Trial group Q1= 0.487, Q3= 0.612, IQR= 0.125 and Median=0.563. Saline group Q1=0.267, Q3=0.329, IQR=0.062, Median=0.317. C5 Deficient group Q1=0.192, Q3=0.278, IQR=0.086, Median=0.268. Data was analyzed using a Kruskal-Wallis test and a Mann-Whitney test to compare each of the groups; ^{o}outliers of ±1.5 IQR from the median, *P≤0.05. Red line separates historical C5 deficient and saline groups from current trial group.

Table 16: Kruskal-Wallis Test for Total Airway Resistance of Trial, Saline, C5 Deficient

Ranks

	Group	N	Mean Rank
TotalAirwayResistance	Trial	12	16.33
	Saline Treated	5	6.60
	C5 Deficient	5	4.80
	Total	22	

Test Statisticsa,b

	TotalAirwayResistance
Chi-square	14.818
df	2
Asymp. Sig.	.001

Table 16: Kruskal-Wallis test for total airway resistance of Trial (n=12), Saline (n=5), C5 Deficient (n=5) groups demonstrated statistically significant difference between the groups (p = 0.001).

Table 17: Mann-Whitney Test

Ranks

	Group	N	Mean Rank	Sum of Ranks
TotalAirwayResistance	Trial	12	11.42	137.00
	C5 Deficient	5	3.20	16.00
	Total	17		

Test Statisticsb

	TotalAirwayResistance
Mann-Whitney U	1.000
Wilcoxon W	16.000
Z	-3.057
Asymp. Sig. (2-tailed)	.002
Exact Sig. [2*(1-tailed Sig.)]	.001

Table 17: Mann-Whitney test for total airway resistance of Trial (n=12) and C5 Deficient (n=5) groups demonstrated statistically significant difference between the groups (p = 0.002).

Table 18: Mann-Whitney

Ranks

	Group	N	Mean Rank	Sum of Ranks
TotalAirwayResistance	Trial	12	11.42	137.00
	Saline Treated	5	3.20	16.00
	Total	17		

Test Statisticsb

	TotalAirwayResistance
Mann-Whitney U	1.000
Wilcoxon W	16.000
Z	-3.057
Asymp. Sig. (2-tailed)	.002
Exact Sig. [2*(1-tailed Sig.)]	.001

Table 18: Mann-Whitney test for total airway resistance of Trial (n=12) and Saline (n=5) groups demonstrated statistically significant difference between the groups (p = 0.002).

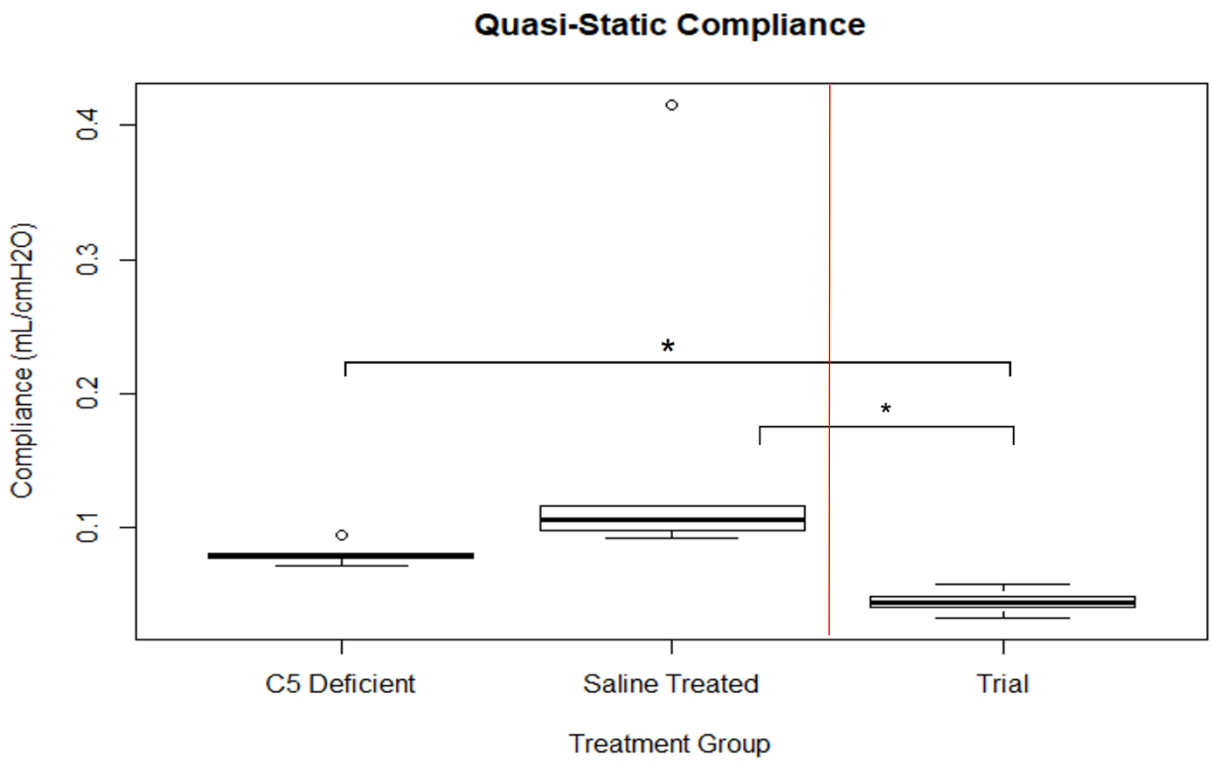

Figure 14: Mice transplanted with C5 competent donor bone marrow (termed trial mice) demonstrate decreased lung compliance when compared to C5 deficient donor bone marrow recipient mice ($p = 0.02$) and saline treated mice ($p = 0.02$). Sub-lethally irradiated BALB/c($Qa2^-$) mice were transplanted with $2x10^6$ spleen cells and $1x10^6$ bone marrow cells from C5 competent or C5 deficient donors or saline. On day 60 post-transplant, a mechanical ventilator was used to measure lung compliance. Data represents 1-5 independent experiments, results from which were pooled for each respective treatment group. Trial group (n=3, 2, 1, 3, 3), C5 deficient transplant group (n=5), and saline group (n=5). Trial group Q1=0.0415, Q3=0.0479, IQR=0.006, Median=0.044. Saline group Q1=0.098, Q3=0.117, IQR=0.018, Median=0.106. C5 Deficient group Q1=0.077, Q3=0.081, IQR=0.004, Median=0.079. Data was analyzed using a Kruskal-Wallis test and a Mann-Whitney test to compare each of the groups; °outliers of ±1.5 IQR from the median, *P≤0.05. Red line separates historical C5 deficient and saline groups from current trial group.

Table 19: Kruskal-Wallis for Compliance of Trial, Saline, C5 Deficient

Ranks

	Group	N	Mean Rank
Compliance	Trial	12	6.50
	Saline Treated	5	19.80
	C5 Deficient	5	15.20
	Total	22	

Test Statisticsa,b

	Compliance
Chi-square	16.907
df	2
Asymp. Sig.	.000

Table 19: Kruskal-Wallis test for lung compliance of Trial (n=12), Saline (n=5), C5 Deficient (n=5) groups demonstrated statistically significant difference between the groups (p = 0.000). P value is shortened to three decimal places in graph but true P value is 0.0002.

Table 20: Mann-Whitney Test

Ranks

	Group	N	Mean Rank	Sum of Ranks
Compliance	Trial	12	11.42	137.00
	Saline Treated	5	3.20	16.00
	Total	17		

Test Statisticsb

	Compliance
Mann-Whitney U	1.000
Wilcoxon W	16.000
Z	-3.057
Asymp. Sig. (2-tailed)	.002
Exact Sig. [2*(1-tailed Sig.)]	.001

Table 20: Mann-Whitney test for lung compliance of Trial (n=12) and Saline (n=5) groups demonstrated statistically significant difference between the groups (p = 0.002).

Table 21: Mann-Whitney Test

Ranks

	Group	N	Mean Rank	Sum of Ranks
Compliance	Trial	12	11.42	137.00
	C5 Deficient	5	3.20	16.00
	Total	17		

Test Statisticsb

	Compliance
Mann-Whitney U	1.000
Wilcoxon W	16.000
Z	-3.057
Asymp. Sig. (2-tailed)	.002
Exact Sig. [2*(1-tailed Sig.)]	.001

Table 21: Mann-Whitney test for lung compliance of Trial (n=12) and Saline (n=5) groups demonstrated statistically significant difference between the groups (p = 0.002).

LentiCRISPR Vectors Were Developed to Knockout Expression of C5 in Murine Bone Marrow Cells as a Potential Treatment for GvHD

In order to create lentiCRISPR vectors capable of knocking out the murine C5 gene three separate sgRNA sequences were provided by Dr. Samuel Workenhe in Dr. Mossman's lab, McMaster University, each targeting their own specific regions in the murine C5 gene (Table 22). Sequences were annealed and incorporated, via digestion and ligation, into their own lentiCRISPRv2 vectors, then transformed into E. coli and grown up by Dr. Workenhe. Plasmids were extracted and purified from E. coli using a PuroLink HiPure Plasmid Midi-Prep kit from Invitrogen (Cat#K210004) by Ekaterina Todorova. The purified plasmid DNA was sent for sequencing to ensure proper integration of sgRNA sequences into the plasmid. Following positive sequencing results the purified plasmid was co-transfected with a packaging, PMDG2, and envelope plasmid, PSPAX2, to produce lentiviral particles in HEK 293T cells by Dr. Workenhe.

Table 22: LentiCRISPR sgRNA Sequences

sgRNA #	Direction	sgRNA sequence
sgRNA 1	FWD	CACCGCCTGGACAAAACTTGGGGAC
	REV	AAACGTCCCCAAGTTTTGTCCAGGC
sgRNA 2	FWD	CACCG ATTTTCCTGGACAAAACTTG
	REV	AAACCAAGTTTTGTCCAGGAAAATC
sgRNA 3	FWD	CACCGAATTTTCCTGGACAAAACTT
	REV	AAACAAGTTTTGTCCAGGAAAATTC

Table 22: Three separate sgRNA sequences each targeting their own specific regions in the murine C5 gene. Sequences are located in the first exon of the *Mus musculus* Hc gene at bases 50-100. Sequences were incorporated into their own lentiCRISPRv2 vectors to later generate viral particles and knockout C5 function.

Co-Transfection of LentiCRISPR Vectors, PMDG2 Vector and PSPAX2 Vector to Produce Lentiviral Particles in HEK 293T Cells

The following steps were performed by Dr. Workenhe individually for each of the three lentiCRISRPv2 vectors previously generated. One hour before the transfection, medium of HEK 293T cells in T150 was changed with 10 ml of optimem. 2.5ml of optimem media was added to a 15 ml falcon tube. In the same tube 100 µl of plus reagent and 10 µg of the lentiCRISPR plasmid were added along with 5 µg of PMDG2 and 7.5 µg of PSPAX2. In another 15 ml falcon tube 2.5 ml of optimem media was added. In the same tube 50 µl of Lipofectamine 2000 was added. Both tubes were incubated for 5 minutes at room temperature and then the Lipofectamine/optimem mix was transferred to the tube containing the DNA and plus reagent. They were mixed gently and the contents were incubated for 25 minutes before the transfection mixture was added to the HEK 293T cells in T150 mentioned above. Once the transfection mixture was added to the flask

of HEK 293T cells it was mixed via gentle rocking and the cells were place back into a 37 degrees Celsius, 5% in air CO_2 incubator for six hours. Following the six hour incubation period the medium was changed to DMEM with 10% Fetal Bovine Serum (FBS), no Penicillin-Streptomycin (P/S) and 1% N,O-bis(trimethylsilyl)acetamide (BSA) and 1x L-Glutamine. 60 hours after transfection the supernatant was harvest and filtered through a 0.45 μM low protein-binding filter (Millipore steriflip HV/PVDF) and then centrifuged at 1008 RCF for 10 minutes by Ekaterina Todorova. Supernatant containing viral particles was then aliquoted and stored at -80 degrees Celsius.

Working concentration of 0.5 μg/ml of Puromycin is Appropriate for Selection of Transduced Murine Bone Marrow Cells

In order to determine the optimal puromycin concentration for selection of transduced cells a puromycin kill curve was conducted on whole bone marrow from DR4, 8 week old female mice. Bone marrow samples were thawed in a 37 degrees Celsius water bath until almost completely liquid. They were added to a 50ml conical tube containing 8ml of pre-warmed media consisting of RPMI, 10% fetal bovine serum (FBS), 100IU/mL penicillin - 100 μg/mL streptomycin (P/S) and 2mM L-glutamine (L-Glut). Cell suspension was centrifuged at 189 RCF for 10 minutes supernatant was discarded. Cell pellet was re-suspended in 15ml of pre-warmed media and added to a flask and placed in a 37 degrees Celsius, 5% in air CO_2 incubator for two hours. After time elapsed, cells were counted using the countess automatic cell counter and $1x10^6$ bone marrow cells were transferred to each of the 6 wells on a 6 well plate and media was

added to a final volume of 2ml in each well. Various concentrations of puromycin, ranging from 0.2 µg/ml to 1 µg/ml, were added to the different wells. Viability was then assessed 24 hrs, 48 hrs, and 72 hrs post-puromycin addition. The 0.5 µg/ml concentration was the lowest concentration that achieved nearly one hundred percent death of wildtype bone marrow cells, 72 hrs- post addition (Table 23).

Table 23: Puromycin Kill Curve of Wildtype Untreated Murine Bone Marrow

Puromycin Concentration	BM Cell Count	Viability (%) After 24 hrs	Viability (%) After 48 hrs	Viability (%) After 72 hrs
0.2 µg/ml	$1x10^6$	71	56	44
0.5 µg/ml	$1x10^6$	53	28	6
1 µg/ml	$1x10^6$	13	0	0

Table 23: Puromycin kill curve for murine BM cells. The 0.5 µg/ml concentration was the lowest concentration that achieved nearly one hundred percent death of wildtype bone marrow cells, 72 hrs- post addition.

In Vitro LentiCRISPR Treatment of BM Cells Produces High Transduction Rates

In order to determine the transduction rate of whole bone marrow with a mixture of the three lentiCRISPR vectors developed, puromycin selection was performed. Previous experimental results conclude that a 0.5 µg/ml concentration of puromycin was most effective for selection of transduced bone marrow cells. Bone marrow samples from DR4, 8 week old female mice were thawed in a 37 degrees Celsius water bath until almost completely liquid. They were added to a 50ml conical tube containing 8ml of pre-warmed media consisting of RPMI,

10% fetal bovine serum (FBS), 100IU/mL penicillin - 100µg/mL streptomycin (P/S) and 2mM L-glutamine (L-Glut). The cell suspension was centrifuged at 189 RCF for 10 minutes supernatant was discarded. The cell pellet was re-suspended in 15ml of pre-warmed media and added to a flask and placed in a 37 degrees Celsius, 5% in air CO_2 incubator for two hours. Following the incubation an equal part mixture of the three lentiCRISPR viral particles was to a 6 well plate containing $1x10^6$ bone marrow cells in 2ml of media. Cells and viral particle mixtures were placed in a 37 degrees Celsius, 5% in air CO_2 incubator for six hours. Cells were then centrifuged at 189 RCF for 10 minutes supernatant was discarded and 2ml of fresh media was added. Puromycin was added at a concentration of 0.5 µg/ml to both wells that contained control or treated cells. Viability was then assessed 24 hrs, 48 hrs, and 72 hrs post-puromycin addition. Seventy two hours post-puromycin selection lentiCRISPR treated cells had a viability of 52% while control bone marrow cells had a viability of 9%. This indicated a transduction efficiency in bone marrow cells of approximately 52% (Table 24).

Table 24: Puromycin Selection of LentiCRISPR Treated Murine Bone Marrow

Treatment	Puromycin Concentration	BM Cell Count	Viability %) After 24 hrs	Viability %) After 48 hrs	Viability %) After 72 hrs
LentiCRISPR	0.5 µg/ml	$1x10^6$	73	54	52
Control	0.5 µg/ml	$1x10^6$	39	16	9

Table 24: Puromycin selection of transduced murine BM cells with lentiCRISPR vector. Transduction efficiency of 52% is seen at 72 hours with variability of 8%.

LentiCRISPR Vector Generated Knockout of C5 in Donor Bone Marrow May be a Promising Potential Treatment for GvHD

To assess the in vivo efficacy of the lentiCRISPR vectors developed the vectors were tested in the previously described murine model of GvHD. As in the previous trial establishing the efficacy of the murine model of GvHD, spleen and bone marrow cells were then harvested from C5 competent (B10.D2-Hc^1 $H2^d$ H2-$T18^c$ /nSnJ Jackson Laboratory). Bone marrow cells were harvested from the femur and tibias of donor mice via grinding with a mortar and pestle in phosphate-buffered saline (PBS) and then filtered through a 70μm cell strainer. Spleen cells were harvested from the donor spleen by rupturing it with a 1mL syring in a petri dish containing 5mL of PBS. Spleen suspension was then filtered through a 40μm strainer. Both spleen and bone marrow cells were processed using Ammonium-Chloride-Potassium (ACK) lysis buffer to lyse and remove red blood cells (RBC) and washed twice with 10mL PBS. Processed bone marrow cells were placed in a 37 degree, 5% in air CO_2 incubator to rest for one hour while spleen cells were stored at four degrees Celsius. Following rest, half of the bone marrow cells were treated with a mixture of all three lentiCRISPR viral particles developed, at equal concentrations, with a final concentration of viral supernatant of 5ml/$4x10^6$ BM cells for the lentiCRISPR group and 5ml/$1x10^6$ BM cells for the 4x lentiCRISPR group. After the addition of the virus mixture the virus and bone marrow cells were left to incubate together in a 37 degree Celsius, 5% in air CO_2 incubator for six hours. The second half of the bone marrow cells were not treated and instead kept as controls in 37 degree Celsius, 5% in air CO_2 incubator until time of use. Immediately after the treated bone marrow cells were placed to incubate six to eight week-old female complement component C5 competent ($Qa2^-$ BALB/cByJ from Jackson Laboratory) recipient mice were irradiated with 650 RADs. Recipient mice were left to rest and recover in ventilated cages on a heating pad. After the six hour incubation had elapsed spleen and both treated and

control bone marrow cells were counted using the countess automated cell counter and resuspended in 200µl of PBS. Six hours following the sub-lethal irradiation recipient mice were transplanted, under isofurane gaseous anesthesia, via retro-orbital (RO) injection with $2x10^6$ spleen cells and either $2x10^6$ treated or $2x10^6$ untreated bone marrow (BM) cells from donor mice. Mice were then maintained in an ultraclean level 2 housing for the first two weeks following the transplant and then transferred to clean vent housing for the remaining six weeks. Mice were harvested via euthanasia on day 60 post-transplant to determine whether development of GvHD occurred. Airway physiology was evaluated using FlexiVent automatic ventilator and then compared to age-matched saline treated control mice to assess development of GvHD. Morphological changes in the lungs were assessed using histological staining techniques for both treatment and control mice and the two groups were compared.

Murine Model of GvHD Transplanted with LentiCRISPR Treated Bone Marrow Leads to Reduction in Disease Severity

To assess the in vivo efficacy of the lentiCRISPR vectors developed and the effects a reduction of donor derived C5 may have on development and severity of GvHD the vectors were tested in the murine model described above. Recipient mice were each transplanted with $2x10^6$ bone marrow cells treated with viral supernatant at a concentration of 5ml/$4x10^6$BM cells and $2x10^6$ spleen cells. This treatment group was titled lentiCRISPR. The control group of mice was transplanted according to the protocol described above in section 2.10, without the addition of lentiCRISPR viral supernatant, and each mouse received $2x10^6$ bone marrow cells and $2x10^6$ spleen cells. Mice were sacrificed at day 60 post-transplant and airway physiology was assessed

using Flexivent. Kruskal-Wallis test performed to compare the total airway resistance of the control group, lentiCRISPR treatment group and the saline group demonstrated a significant difference ($p = 0.005$) (Table 25). Subsequently a Mann-Whitney test was run between each group to determine where any significant differences lie. Using this test significance was demonstrated between the lentiCRISPR group had significantly lower total airway resistance when compared to the control group with a p value of 0.05 (Figure 15 & Table 26). Significance was also demonstrated between the saline treatment group and the lentiCRISPR treatment group ($p = 0.014$) with the saline group having lower total airway resistance (Figure 15 & Table 27). Finally using the same test, significance was noted between the saline group and the control group ($p = 0.009$) (Table 28).

When comparing the lung compliance between the lentiCRISPR, saline and control groups statistical significance was seen using the Kruskal-Wallis test ($p = 0.004$) (Table 29). The Mann-Whitney test for compliance data of the control and lentiCRISPR groups shows the lentiCRISPR group to have significance higher lung compliance with a p value of 0.05 (Figure 16 & Table 30). A subsequent Mann-Whitney test for compliance data between the lentiCRISPR and saline groups shows that lentiCRISPR group has significantly lower compliance than the saline group at a p value of 0.014 (Figure 16 & Table 31).

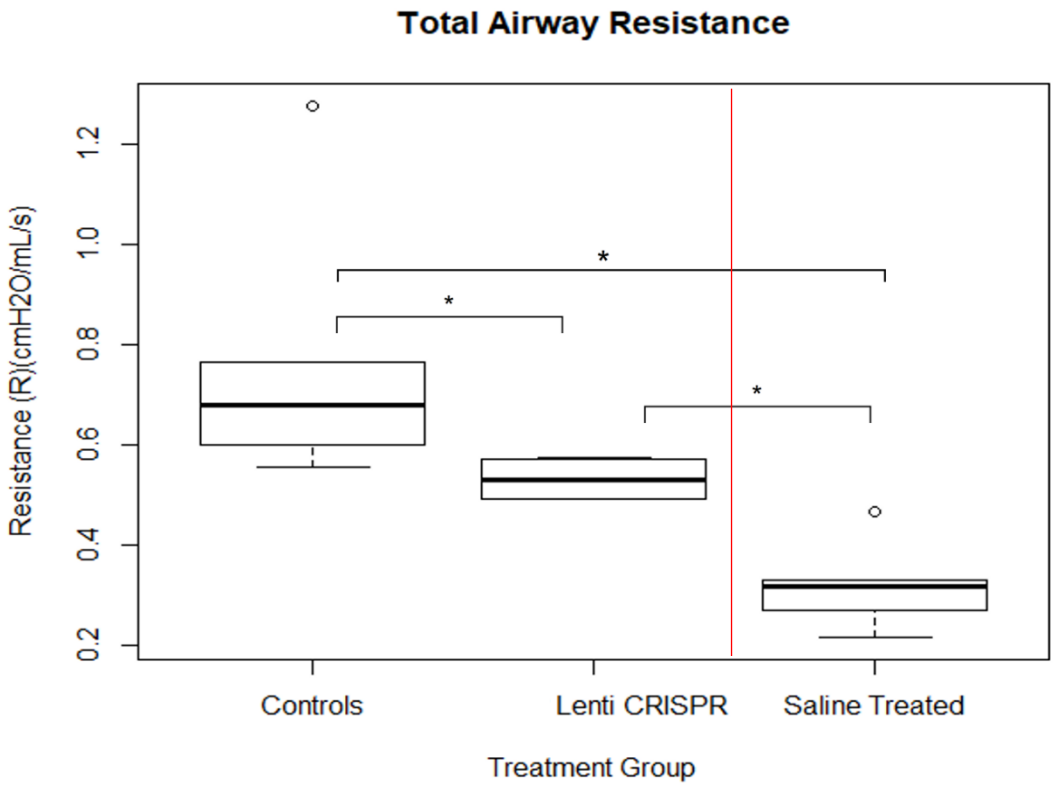

Figure 15: Mice transplanted with lentiCRISPR treated bone marrow demonstrate decreased total airway resistance when compared to the control group ($p = 0.05$) and increased total airway resistance compared to the saline group ($p = 0.014$). Sub-lethally irradiated BALB/c($Qa2^-$) mice were transplanted with $2x10^6$ spleen cells and $2x10^6$ lentiCRISPR treated or untreated bone marrow cells or saline. On day 60 post-transplant, a mechanical ventilator was used to measure total airway resistance. Data represents 1-2 independent experiments, results from which were pooled for each respective treatment group. LentiCRISPR treated transplant group (n=4), control group (n=3,2), and saline group (n= 5). LentiCRISRP group Q1=0.493, Q3=0.569, IQR=0.076, Median=0.531.Saline group Q1=0.267, Q3=0.329, IQR=0.062, Median=0.317. Control group Q1=0.601, Q3=0.764, IQR=0.163, Median=0.679. Data was analyzed using a Kruskal-Wallis test and a Mann-Whitney test to compare each of the groups; °outliers of ±1.5 IQR from the median,*P≤0.05. Red line separates historical saline group from current groups of controls and lentiCRISPR.

Table 25: Kruskal-Wallis Test for lentiCRISPR, saline, control

Ranks

	Comparison	N	Mean Rank
TotalAirwayResistance	Saline Treated	5	3.00
	Lenti CRISPR	4	8.00
	Controls	5	11.60
	Total	14	

Test Statisticsa,b

	TotalAirwayResistance
Chi-square	10.646
df	2
Asymp. Sig.	.005

Table 25: Kruskal-Wallis test for total airway resistance of lentiCRIPSR, Saline and Control groups demonstrated statistically significant difference between the groups (p = 0.05).

Table 26: Mann-Whitney test

Ranks

	Group	N	Mean Rank	Sum of Ranks
TotalAirwayResistance	Lenti CRISPR	4	3.00	12.00
	Controls	5	6.60	33.00
	Total	9		

Test Statisticsb

	TotalAirwayResistance
Mann-Whitney U	2.000
Wilcoxon W	12.000
Z	-1.960
Asymp. Sig. (2-tailed)	.050
Exact Sig. [2*(1-tailed Sig.)]	.063

Table 26: Mann-Whitney test for total airway resistance of lentiCRISPR and Control groups demonstrated statistically significant difference between the groups (p = 0.05).

Table 27: Mann-Whitney test

Ranks

	Group	N	Mean Rank	Sum of Ranks
TotalAirwayResistance	Saline Treated	5	3.00	15.00
	Lenti CRISPR	4	7.50	30.00
	Total	9		

Test Statisticsb

	TotalAirwayResistance
Mann-Whitney U	.000
Wilcoxon W	15.000
Z	-2.449
Asymp. Sig. (2-tailed)	.014
Exact Sig. [2*(1-tailed Sig.)]	.016

Table 27: Mann-Whitney test for total airway resistance of lentiCRISPR and Saline groups demonstrated statistically significant difference between the groups (p = 0.014).

Table 28: Mann-Whitney test

Ranks

	Group	N	Mean Rank	Sum of Ranks
TotalAirwayResistance	Saline Treated	5	3.00	15.00
	Controls	5	8.00	40.00
	Total	10		

Test Statisticsb

	TotalAirwayResistance
Mann-Whitney U	.000
Wilcoxon W	15.000
Z	-2.611
Asymp. Sig. (2-tailed)	.009
Exact Sig. [2*(1-tailed Sig.)]	.008

Table 28: Mann-Whitney test for total airway resistance of Saline and Control groups demonstrated statistically significant difference between the groups (p = 0.009).

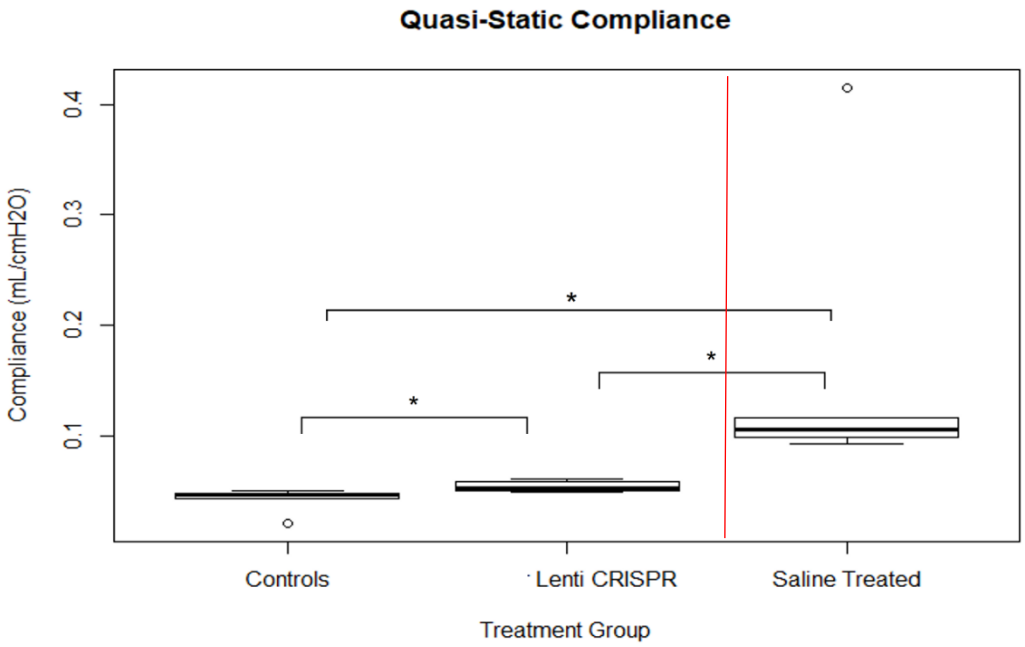

Figure 16: Mice transplanted with lentiCRISPR treated bone marrow demonstrate an increase in lung compliance (p = 0.05) when compared to the control group and lower lung compliance when compared to the saline group (p = 0.014). Sub-lethally irradiated BALB/c(Qa2$^-$) mice were transplanted with 2x10^6 spleen cells and 2x10^6 lentiCRISPR treated or untreated bone marrow cells or saline. On day 60 post-transplant, a mechanical ventilator was used to measure lung compliance. Data represents 1-2 independent experiments, results from which were pooled for each respective treatment group. LentiCRISPR treated transplant group (n=4), control group (n=3,2), and saline group (n=5). LentiCRISPR group Q1=0.0496, Q3=0.0566, IQR=0.007, Median=0.0525. Saline group Q1=0.098, Q3=0.117, IQR=0.018, Median=0.106. Control group Q1=0.042, Q3=0.047, IQR=0.005, Median=0.046. There is a significant difference between the lentiCRISPR treated and control groups, as well as between the lentiCRISPR treated and saline groups. Data was analyzed using a Kruskal-Wallis test and a Mann-Whitney test to compare each of the groups; °outliers of ±1.5 IQR from the median, *P≤0.05. Red line separates historical saline group from current groups of controls and lentiCRISPR.

Table 29: Kruskal-Wallis Test for lentiCRISPR, saline, control

Ranks

	Comparison	N	Mean Rank
Compliance	Saline Treated	5	12.00
	Lenti CRISPR	4	7.25
	Controls	5	3.20
	Total	14	

Test Statisticsa,b

	Compliance
Chi-square	11.083
df	2
Asymp. Sig.	.004

Table 29: Kruskal-Wallis test for lung compliance of lentiCRISPR, Saline and Control groups demonstrated statistically significant difference between the groups (p = 0.04).

Table 30: Mann-Whitney Test

Ranks

	Group	N	Mean Rank	Sum of Ranks
Compliance	Lenti CRISPR	4	3.00	12.00
	Controls	5	6.60	33.00
	Total	9		

Test Statisticsb

	Compliance
Mann-Whitney U	2.000
Wilcoxon W	12.000
Z	-1.960
Asymp. Sig. (2-tailed)	.050
Exact Sig. [2*(1-tailed Sig.)]	.063

Table 30: Mann-Whitney test for lung compliance of lentiCRISPR and Control groups demonstrated statistically significant difference between the groups (p = 0.05).

Table 31: Mann-Whitney Test

Ranks

	Group	N	Mean Rank	Sum of Ranks
Compliance	Saline Treated	5	3.00	15.00
	Lenti CRISPR	4	7.50	30.00
	Total	9		

Test Statisticsb

	Compliance
Mann-Whitney U	.000
Wilcoxon W	15.000
Z	-2.449
Asymp. Sig. (2-tailed)	.014
Exact Sig. [2*(1-tailed Sig.)]	.016

Table 31: Mann-Whitney test for lung compliance of lentiCRISPR and Saline groups demonstrated statistically significant difference between the groups (p = 0.014).

Histologically Assessed Changes in Airway Morphology Imply Decreased Disease Severity in lentiCRISPR treated BM recipient Mice

Fibrosis represents a key parameter of GvHD and it was assessed using histological staining of mouse lung airway to identify changes in fibrotic deposits signaling development of GvHD. At day 60 post-transplant mouse lungs were harvest and the left lobe of each lung taken for histological study. The lobe was inflated using 10% formalin as a fixative, at a pressure of 20cm H20 and once inflated it was submerged in 10% formalin for 48 hours. Following the 48 hour fixation period the lung was sectioned into superior, middle and inferior sections and transferred to 70% ethanol to halt the fixation process. Lung tissues were then embedded in paraffin wax and cut into 5μm sections and stained with hematoxylin and eosin and Masson's trichrome blue. Images of stained slides were capture using Olympus bright-field microscope at various resolutions (Figure 17).

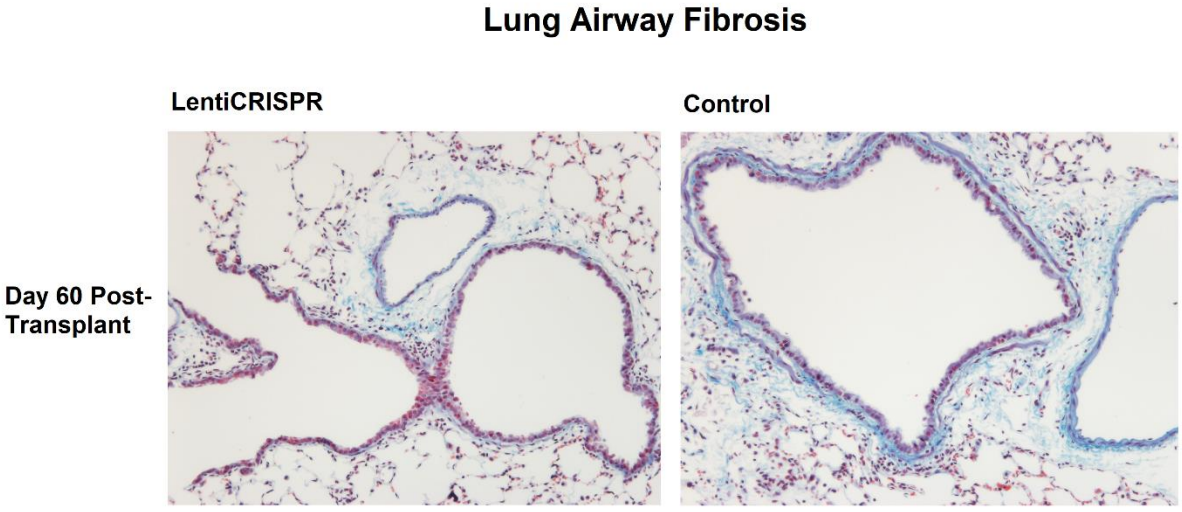

Figure 17: Murine lungs were harvested from lentiCRISPR treated and control mice and fixed in 10% formalin for 48 hours, paraffin embedded and sectioned. Sections were stained with Masson's Trichrome Blue and Eosin. Increased levels of fibrosis can be seen surrounding the airway in the control group when compared to the lentiCRISPR group.

Alternate Statistical Analysis of Ventilator Derived Data for lentiCRISPR Group Demonstrated Reduction in Disease Severity in Lung Compliance but Not in Total Airway Resistance

In previous statistical analyses all mice in each treatment group were included. Although the sample size of the treatment groups is too low to be able to determine outliers with confidence, for thoroughness, the same statistical analyses were run but excluding mice that had total airway resistance or lung compliance values that differed by 1.5 of the interquartile range (IQR) away from the median. A Kruskal-Wallis test demonstrated a statistically significant difference between lentiCRISPR, Saline and Control groups ($p = 0.06$) (Table 32).With the exclusion of these potential outliers there is no statistically significant difference between the total airway resistance values of the lentiCRISPR and control groups ($p = 0.083$, Figure 19 & Table 35). There is however, a statistically significant difference in the lung compliance levels between the lentiCRISPR treated and control groups ($p = 0.043$), with lentiCRISPR having higher lung compliance levels than controls (Figure 18 & Table 33). There is also a statistically significant difference seen, when potential outliers are removed, between the Trial and lentiCRISPR groups ($p = 0.029$), with the lentiCRISPR group having higher lung compliance than the trial (Table 34).

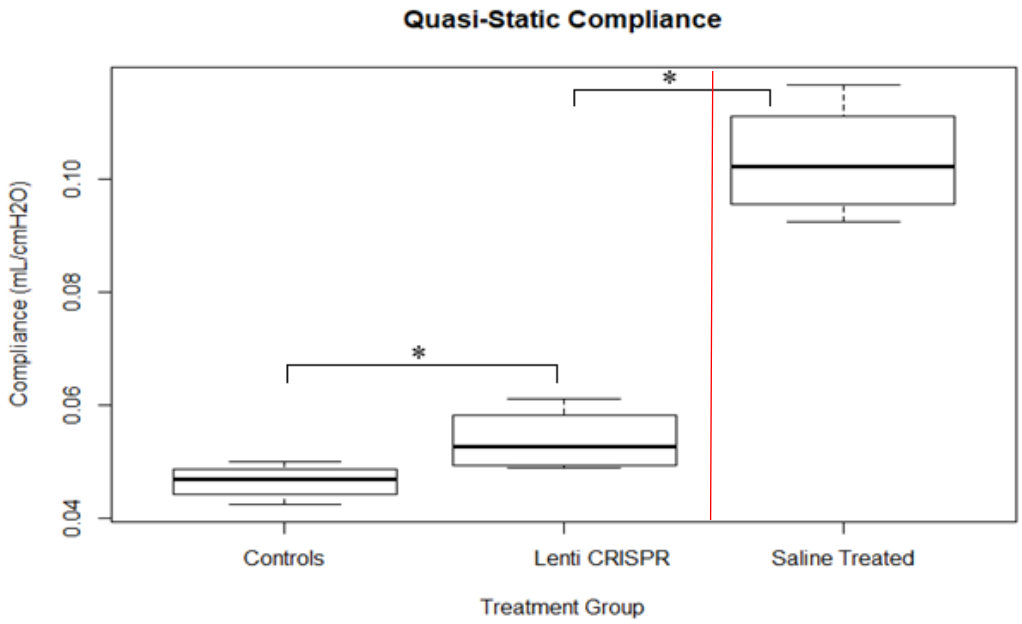

Figure 18: Mice transplanted with lentiCRISPR treated bone marrow demonstrate an increase in lung compliance (p = 0.043) when compared to the control group. Sub-lethally irradiated BALB/c(Qa2$^-$) mice were transplanted with 2x10^6 spleen cells and 2x10^6 lentiCRISPR treated or untreated bone marrow cells or saline. On day 60 post-transplant, a mechanical ventilator was used to measure lung compliance. Data represents 1-2 independent experiments, results from which were pooled for each respective treatment group. LentiCRISPR treated transplant group (n=4), control group (n=2,2), and saline group (n= 5). LentiCRISPR group Q1=0.0496, Q3=0.0566, IQR=0.007, Median=0.0525. Saline group Q1=0.097, Q3=0.108, IQR=0.011, Median=0.102. Control group Q1=0.045, Q3=0.048, IQR=0.003, Median=0.047. There is a significant difference between the lentiCRISPR treated and control groups, as well as between the lentiCRISPR treated and saline groups. Data was analyzed using a Kruskal-Wallis test and a Mann-Whitney test to compare each of the groups. Outliers of ±1.5 IQR from the median have been removed from data set; *P≤0.05. Red line separates historical saline group from current groups of controls and lentiCRISPR.

Ranks

	Comparison	N	Mean Rank
Compliance	Saline Treated	5	11.00
	LentiCRISPR	4	6.25
	Controls	4	2.75
	Total	13	

Test Statisticsa,b

	Compliance
Chi-square	10.187
df	2
Asymp. Sig.	.006

Table 32: Kruskal-Wallis test for lung compliance of lentiCRISPR, Saline and Control groups demonstrated statistically significant difference between the groups (p = 0.006).

Table 33: Mann-Whitney Test

Ranks

	Group	N	Mean Rank	Sum of Ranks
Compliance	Lenti CRISPR	4	6.25	25.00
	Controls	4	2.75	11.00
	Total	8		

Test Statisticsb

	Compliance
Mann-Whitney U	1.000
Wilcoxon W	11.000
Z	-2.021
Asymp. Sig. (2-tailed)	.043
Exact Sig. [2*(1-tailed Sig.)]	.057

Table 33: Mann-Whitney test for lung compliance of lentiCRISPR and Control groups demonstrated statistically significant difference between the groups (p = 0.043).

Table 34: Mann-Whitney Test

Ranks

	Group	N	Mean Rank	Sum of Ranks
Compliance	Trial	12	7.00	84.00
	Lenti CRISPR	4	13.00	52.00
	Total	16		

Test Statisticsb

	Compliance
Mann-Whitney U	6.000
Wilcoxon W	84.000
Z	-2.183
Asymp. Sig. (2-tailed)	.029
Exact Sig. [2*(1-tailed Sig.)]	.030

Table 34: Mann-Whitney test for lung compliance of lentiCRISPR and Trial groups demonstrated statistically significant difference between the groups (p = 0.029).

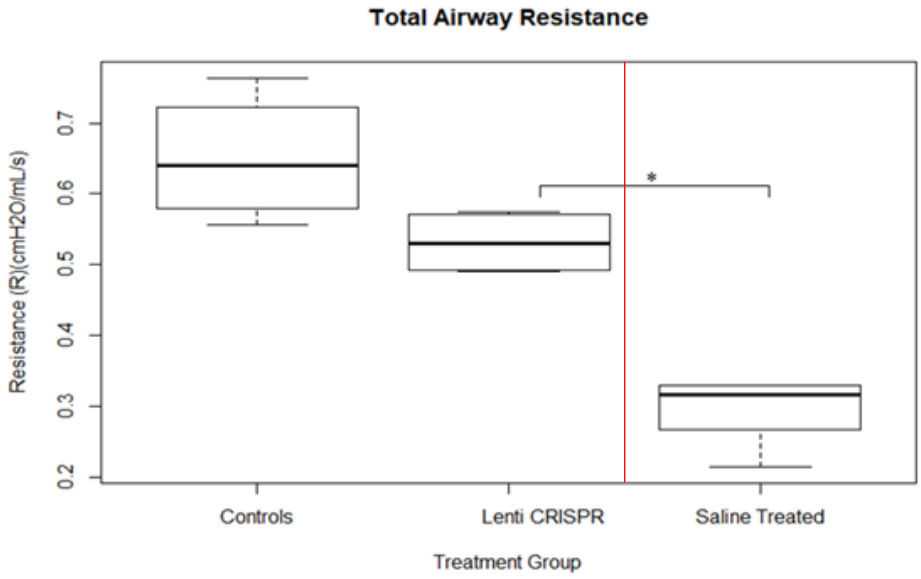

Figure 19: Mice transplanted with lentiCRISPR treated bone marrow demonstrate no significant difference in total airway resistance when compared to the control group (p = 0.83). Sub-lethally irradiated BALB/c(Qa2$^-$) mice were transplanted with 2x10^6 spleen cells and 2x10^6 lentiCRISPR treated or untreated bone marrow cells or saline. On day 60 post-transplant, a mechanical ventilator was used to measure lung compliance. Data represents 1-2 independent experiments, results from which were pooled for each respective treatment group. LentiCRISPR treated transplant group (n=4), control group (n=2,2), and saline group (n=5). LentiCRISRP group Q1=0.493, Q3=0.569, IQR=0.076, Median=0.531.Saline group Q1=0.267, Q3=0.329, IQR=0.062, Median=0.317. Control group Q1=0.589, Q3=0.700, IQR=0.111, Median=0.640. Data was analyzed using a Kruskal-Wallis test and a Mann-Whitney test to compare each of the

groups. Outliers of ±1.5 IQR from the median have been removed from data set; *P≤0.05. Red line separates historical saline group from current groups of controls and lentiCRISPR.

Ranks

	Group	N	Mean Rank	Sum of Ranks
TotalAirwayResistance	Lenti CRISPR	4	3.00	12.00
	Controls	4	6.00	24.00
	Total	8		

Test Statisticsb

	TotalAirwayResistance
Mann-Whitney U	2.000
Wilcoxon W	12.000
Z	-1.732
Asymp. Sig. (2-tailed)	.083
Exact Sig. [2*(1-tailed Sig.)]	.114

Table 35: Mann-Whitney test for total airway resistance of lentiCRISPR and Control groups demonstrated no statistically significant difference between the groups (p = 0.083).

3.0 Discussion and Limitations

Fibrosis is a sign of a number of disease states and being able to accurately determine fibrosis levels in the airways of the lungs of a patient is key for providing appropriate treatment [77]. Total airway resistance can be taken as a surrogate measure of the level of obstruction in the lungs, such as fibrosis [78]. With increased fibrosis in the lung airways, the airways become stiffer and more work is required for adequate ventilation to be achieved [79]. On that basis, in this study, measurement of total airway resistance was taken as a means to determine fibrosis levels in the lungs. Comparison between the total airway resistance of the control group and the saline treated group demonstrated a highly significant difference ($p = 0.009$) which suggests that mice in the control group developed GvHD (Table 28). Since increased total airway resistance is a characteristic of the GvHD disease state, a lower total airway resistance value would be indicative of a reduction in disease severity. When tested in vivo in our GvHD mouse model the lentiCRISPR treated mice showed significantly lower total airway resistance when compared to controls ($p = 0.05$) but still higher than the saline treated group (Figures 15 & Table 26). This is indicative of a potential treatment effect that reduces disease severity. The p value of 0.05 is still regarded as significant in common practise but should be viewed as more of a likely trend between the data, rather than an absolute relationship. Although this data suggest a trend of reduction in disease state severity with the lentiCRISPR treatment, it is important to note that p value is on the higher end of the spectrum of significance. This could be due to a number of factors, one of which is the small sample size of the different groups. Repetition of the experiment with a larger sample size would be one way to confirm these findings. It is also important to distinguish the fact that the lentiCRISPR treatment potentially reduced disease severity but did not abolish the disease state in the mice that received the treatment. This can be seen by the significant difference in total airway resistance demonstrated by the Mann-Whitney

test between the lentiCRISPR group and the saline group data (p = 0.014) (Table 27). The saline group, having only received a 200µl injection of saline, acts as a negative control since it is known not to lead to development of GvHD and total airway resistance measurements of that group can be seen as the normal baseline. The lentiCRIPSR treated group however had significantly higher total airway resistance in comparison to that baseline, indicating increased fibrosis in the lungs and presence of GvHD.

Another measure for lung function and obstruction such as fibrosis is compliance [78]. Lung compliance is defined as the change in lung volume per unit change of transpulmonary pressure [80]. It is the distensibility of the lung which can change depending on the physiology of the lung. As lung fibrosis increases the compliance of the lung decreases for a given unit of transpulmonary pressure [80]. This difference in compliance was seen in the data gathered from the lentiCRISPR, saline and control groups that showed a statistically significant difference when analyzed using the Kruskal-Wallis test (p = 0.004) (Table 29). When each group was compared separately using a Mann-Whitney test a significant difference between the lentiCRISPR group and the control group, with a p value of 0.05, the lentiCRISPR group showed significant higher lung compliance (Figure 16 & Table 30). This higher compliance is indicative of lower levels of lung fibrosis in mice treated with the lentiCRISPR treatment. Since lower lung compliance values are associated with the GvHD state, this suggests that the treatment was able to significantly reduce the severity of GvHD in this mouse model. Again, as previously stated the p value is at the higher range and the sample size was small, so a repetition of the experiment would be able to confirm these findings. When compared to the saline treated, negative control, mice, the lentiCRISPR treatment group had significantly lower lung compliance (p = 0.014) (Figure 16 & Table 31). This again leads to the conclusion that the treatment only worked to

reduce GvHD severity in these treatment animals, rather than to prevent or eliminate the disease state all together.

Histological staining of lung tissues collected from lentiCRISPR and control mice also suggest a potential disease reduction due to the lentiCRISPR treatment. The lentiCRISPR group seemed to display lower levels of fibrosis than the control group when qualitatively comparing Masson's Trichrome Blue and Eosin stained sections of lung tissue from both groups (Figure 17).

Although the sample sizes in these experiments are too small to be able to identify outliers with confidence, for thoroughness, a secondary data analysis was conducted that excluded all data points that differed by 1.5 of the interquartile range (IQR) away from the median. Even with potential outliers removed the Mann-Whitney test comparison of lung compliance data between the lentiCRISPR treated and control groups demonstrated that the lentiCRISPR group has significantly higher lung compliance levels when compared to the control group ($p = 0.043$, Figure 18 & Table 33). That again implicates a reduction in disease severity, due to the lentiCRISPR treatment, as higher lung compliance levels are consistent with lower levels of airway stiffness and therefore lower levels of fibrosis. With the exclusion of these potential outliers however, there is no statistically significant difference between the total airway resistance values of the lentiCRISPR and control groups ($p = 0.083$, Figure 19 & Table 35). Due to the small sample sizes however, removal of even one subject can make a large difference in significance between the data.

For thoroughness a comparison was done for lung compliance levels of lentiCRISPR and trial groups using the adjusted data. This was done as a secondary method to verify that significant differences in lung compliance levels between lentiCRISPR treated and control

groups were reliable. It was possible since mice in both the trial and control groups underwent the same procedures and the same protocol was followed. When a Mann-Whitney test was done comparing the adjusted lung compliance data for trial and lentiCRISPR groups, the lentiCRISPR group was shown to have significantly higher lung compliance levels ($p = 0.029$, Table 34).

Limitations

One large limitation to be mindful of is the small sample sizes of the different treatment groups. With these smaller sample sizes the experiment was underpowered and therefore there is a larger possibility of having a Type 1 error, or false positive. Although the lentiCRISPR treatment group had significantly lower resistance and significantly higher compliance levels when compared to the control group, the sample size was too small to be able to conclude that this was a true relationship between the data. In data sets of a small sample size a single point, such as an outlier, would have a greater effect on the skew of the data and therefore on statistical relations between the data sets. That is why the alternative data analysis, excluding the outliers, was conducted. Although following the removal of outliers the lung compliance levels of lentiCRISPR treatment mice remained significantly higher than those of control mice ($p = 0.043$, Figure 18 & Table 33), statistical significance for total airway resistance was lost ($p = 0.083$, Figure 19 & Table 35). The only way to be certain of the validity of these results is to repeat the experiment using a larger sample.

Another factor to consider is the spread of the data for each group. The data sets showed a small spread of the data for each group with individual data points in the group being clustered together. In the non-adjusted data, which includes possible outliers, the lentiCRISPR group lung

compliance had an IQR of 0.062, the saline group had an IQR of 0.062 and the control group had an IQR of 0.163 (Figure 16). Once outliers were removed, in the adjusted data, the lentiCRISPR group had an IQR of 0.007, the saline group had an IQR of 0.018 and the control group had an IQR of 0.005 (Figures 18). This small spread of data in each group is more encouraging for trusting the validity of the results seen but repetition of the experimental conditions with a larger sample size would be a more conclusive way to verify these results.

A statistically relevant difference is seen between the lentiCRISPR treatment group and the controls however, statistical analyses are only valuable when contextualized in a biological setting. Further experiments would be required to define whether this reduction is a biologically relevant one. Repetition of the experimental conditions with the addition of hemolytic assays to determine C5 function at multiple time points throughout the 60 day experimental duration would be one way to define the biological relevance of the treatment.

Historical data was used as a reference point to support the fact that the lentiCRISPR treatment potentially only reduced disease severity rather than abolishing it. This is a limitation because the experiments, although the same procedurally, were carried out at different times and that could add confounding variables. To control for possible confounding variables mice in the historical groups, saline and C5 deficient, as well as all current groups were purchased from the same provider (Jackson laboratories), age matched, housed in the same facility and received the same diet and care. When comparing lung compliance levels between the historical C5 sufficient mice, termed C5+, and the control mice that were treated in the same way there was no statistical difference found ($p = 0.089$, Figure 11 & Table 12). However, the small sample size is still a relevant concern. Future experimentation, where these conditions are repeated and all

experimental groups are initiating at the same time, would be a strong way to validate these results.

Like all animal models, the one used in this study does not fully represent the disease state seen in humans. In this case it is important to note that the miss match responsible for the initiation of the disease is between the minor histocompatibility complexes in the murine model of GvHD while in clinical practise miss-matches between major histocompatibility complexes are monitored [81].

A potential issue is that the murine model utilizes the transfer of donor splenocytes along with donor bone marrow cells which is not seen in bone marrow transplants in humans. The splenocytes are included in the murine model because amongst them there are mature T cells, which are ultimately responsible for the initiation of GvHD. This however is not representative of the procedures in practise for human bone marrow transplant and poses a limitation when attempting to generalize finding to the human presentation or underlying cause of the disease [81]. One positive fact regarding the procedures followed in the murine model of GvHD is that only bone marrow cells were treated and splenocytes were not, yet there was still a significant reduction in disease severity observed in the lentiCRISPR treatment group. This is indicative that donor bone marrow derived cells are also responsible in disease initiation and propagation and downregulation of complement C5 expression may be a potentially useful treatment option.

Another key factor that may pose a limitation is that human bone marrow transplants currently in clinical practise consist of transplantation of pure hematopoietic stem cells (CD34+) and our model transplants whole bone marrows. Not only is this not representative of the human procedure but it also means that the cells that are potentially transduced with lentiCRISPR vectors during treatment conditions are not pluripotent in nature and the genetic modification

they take on will be lost as they die off. Only 1.1% of whole murine bone marrow consists of CD34+ cells [82]. That means that even if one hundred percent of the cells in the whole bone marrow to be transplanted are transduced with the lentiCRISPR vector, then at most 1.1% of the cells will be of self-regenerating nature and will not be lost over time. To correct this future murine experiments should be done with pure CD34+ cells transplanted into the mouse instead of whole bone marrow.

Although previously studied in the literature, the effects of lentiCRISPR vectors on cells is not fully described, leaving the possibility of unknown off-target effects occurring. There is even the possibility that the effects of disease severity reduction seen in this study, may be due to the lentiCRISPR vectors themselves rather than the cleavage and subsequent lack of donor function C5. To address this, future experiments could include an empty vector control, where recipient mice are transplanted with BM cells that have been transduced with a lentiCRISPRv2 vector that is lacking a guide RNA.

The same principles of potential off-target effects accounting for the disease severity reduction seen in this study, apply to the radiation experienced by the recipient mice. To address the possible effects of the applied radiation, a group of synergistic transplants (Blab/c to Blab/c) could be performed. In this group Blab/c recipient mice would be irradiated with 650 RADs and six hours post irradiation they would be transplanted with Blab/c donor mouse BM and spleen cells.

Although it would be assumed that a dose dependent decrease in disease severity would be observed, with the increase in dosage of virus delivered to the bone marrow cells from the lentiCRIPSR group to the 4x lentiCRIPSR group (see Appendix below), that was not the case. Proper comparison between these two experiments cannot be conducted due to human and

mechanical errors that occurred during the execution of the 4x lentiCRIPSR experiment. The incubation time of the bone marrow cells with the virus was decreased from 6 hours to 4.5 hours and may not have allowed for the same transduction rates to be reached. Further mechanical malfunctions in the Countess Cell counter used did not allow for proper cell counts to be taken and the proportion of BM cells to virus would be affected. Since a change of 50% or greater in C5 expression levels is assumed to create a biologically relevant and detectable difference in in vivo experimentation, if less than 50% of the bone marrow cells were transduced with the lentiCRISPR vector then it is unlikely to see a difference in the disease model [83]. This reasoning could help explain why the 4x lentiCRISPR treatment group did not show a significant change in total airway resistance ($p = 1.00$) or lung compliance ($p = 1.00$) when compared to controls (Tables 37 & 40). There was however a significant difference between the saline treated group and the 4x lentiCRISPR group indicating that there was increased total airway resistance ($p = 0.027$) and decreased lung compliance ($p = 0.027$, Tables 38 & 40). All of this data taken together leads to the conclusion that the 4x lentiCRISPR group developed GvHD at a similar severity level as the positive controls. Unfortunately no conclusions can be drawn regarding to the efficacy of this lentiCRISPR dosage due to the shortened incubation time of the bone marrow cells with the viral particles and the malfunctions in the Countess cell counter. Ideally these experimental conditions should be repeated with the proper six hour incubation time, reliable cell counting methods and a larger sample size.

4.0 Appendix

Murine Model of GvHD Transplanted with 4x LentiCRISPR Dose Treated Bone Marrow Developed GvHD

To assess whether the reduction in the severity of GvHD seen in the lentiCRISPR treated group was dose dependent the experimental steps were repeated with four times the viral concentration used in the lentiCRISPR group. However, viral incubation duration and malfunctions in the Countess Cell Counter meant all procedures could not be carried out as in the original lentiCRISPR experiment and results of this experiment are not comparable to mice in the lentiCRISPR group. In the four time viral concentration experiment recipient mice were each transplanted with $1x10^6$ bone marrow cells treated with viral soup for 4.5 hours at a concentration of 5ml/$1x10^6$BM cells and $2x10^6$ spleen cells. This treatment group was titled 4x lentiCRISPR. The control group of mice was transplanted according to the protocol described in section 2.10, without the addition of lentiCRISPR viral soup, and each mouse received $1x10^6$ bone marrow cells and $2x10^6$ spleen cells. Mice were sacrificed at day 60 post-transplant and airway physiology was assessed using Flexivent. Kruskal-Wallis test performed to compare the total airway resistance of the control group, 4x lentiCRISPR treatment group and the saline group and a significance of $p = 0.016$ was seen (Table 36). To determine the specific relation of each group to the other Mann-Whitney tests were run between each group. There was no significance found between the 4x lentiCRISPR group and the control group for total airway resistance with a p value of 1.00 (Figure 20 & Table 37). The total airway resistance for 4x lentiCRISPR treatment group is significantly higher than the saline group ($p = 0.027$, Table 38) Kruskal-Wallis test was done for the compliance data collected for the 4x lentiCRISPR, saline and control groups and a significant difference was found between the groups ($p = 0.011$) (Table 39). Mann-Whitney tests were done for the compliance data between each group and a

significant difference was noted between saline and 4x lentiCRISPR groups at a p value of 0.027 (Figure 21 & Table 40). There was no significant difference found between the 4x lentiCRISPR and control groups (p = 1.00, Table 41).

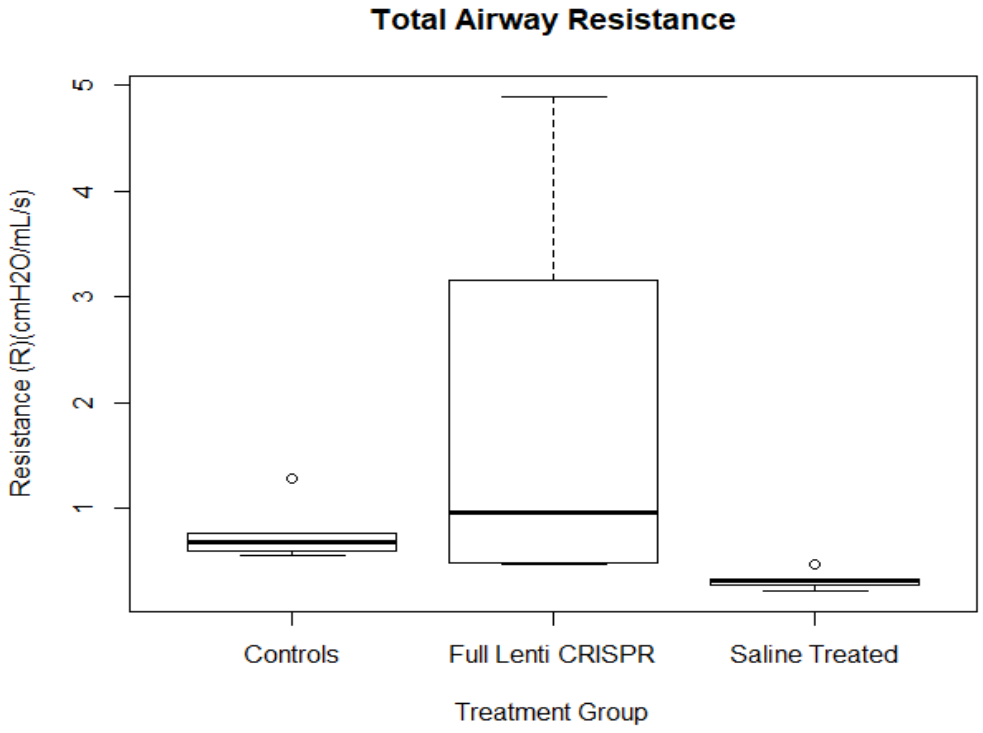

Figure 20: Total airway resistance data compared for Control, 4x lentiCRISPR and Saline Treated groups. 4x lentiCRISPR treatment group show no statistical significance in total airway resistance when compare to the Control group (p = 1.00).

Table 36: Kruskal-Wallis Test for 4x lenti, saline, control

Ranks

	LentiComparison	N	Mean Rank
TotalAirwayResistance	Saline Treated	5	3.20
	4x Lenti CRISPR	4	9.75
	Controls	5	10.00
	Total	14	

Test Statisticsa,b

	TotalAirwayResistance
Chi-square	8.226
df	2
Asymp. Sig.	.016

Table 36: Kruskal-Wallis test for total airway resistance of 4x lentiCRIPSR, Saline and Control groups demonstrated statistically significant difference between the groups (p = 0.016).

Table 37: Mann-Whitney Test

Ranks

	Group	N	Mean Rank	Sum of Ranks
TotalAirwayResistance	4x Lenti CRISPR	4	5.00	20.00
	Controls	5	5.00	25.00
	Total	9		

Test Statisticsb

	TotalAirwayResistance
Mann-Whitney U	10.000
Wilcoxon W	25.000
Z	.000
Asymp. Sig. (2-tailed)	1.000
Exact Sig. [2*(1-tailed Sig.)]	1.000

Table 37: Mann-Whitney test for total airway resistance of 4x lentiCRISPR and Control groups demonstrated no statistically significant difference between the groups (p = 1.00).

Table 38: Mann-Whitney Test

Ranks

	Group	N	Mean Rank	Sum of Ranks
TotalAirwayResistance	Saline Treated	5	3.20	16.00
	4x Lenti CRISPR	4	7.25	29.00
	Total	9		

Test Statisticsb

	TotalAirwayResistance
Mann-Whitney U	1.000
Wilcoxon W	16.000
Z	-2.205
Asymp. Sig. (2-tailed)	.027
Exact Sig. [2*(1-tailed Sig.)]	.032

Table 38: Mann-Whitney test for total airway resistance of 4x lentiCRISPR and Saline groups demonstrated statistically significant difference between the groups (p = 0.027).

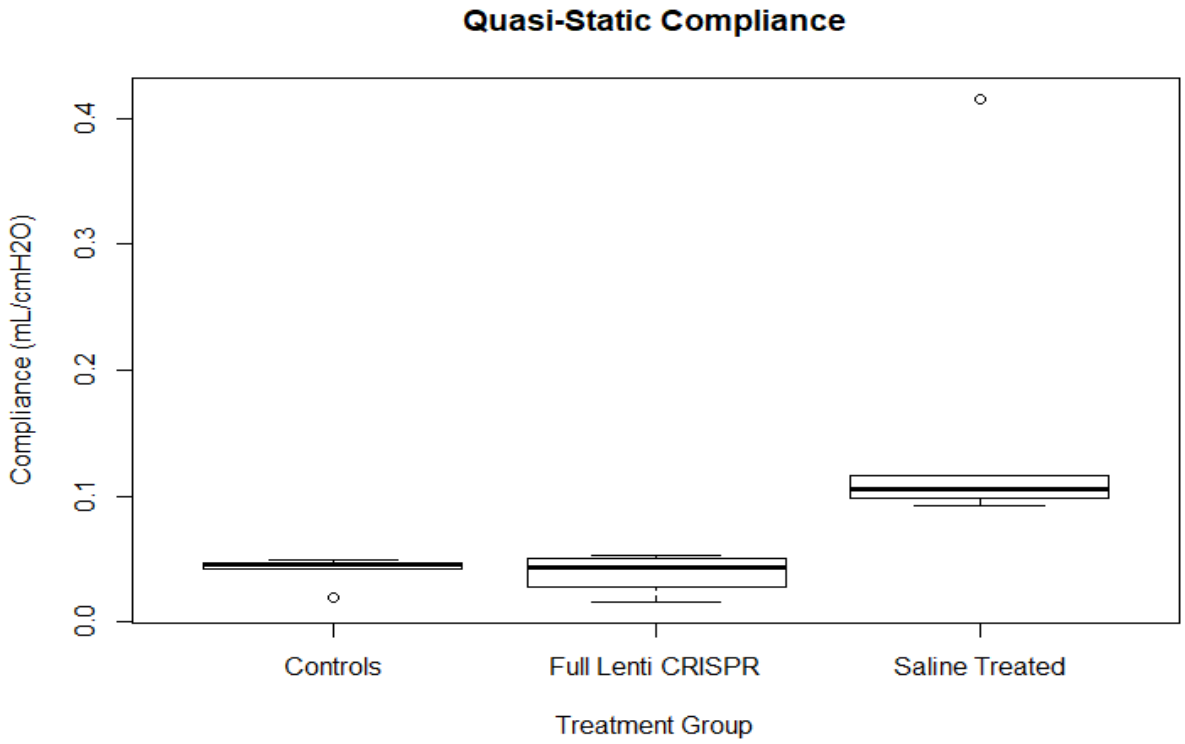

Figure 21: Quasi-Static Compliance data compared for Control, 4x lentiCRISPR and Saline Treated groups. 4x lentiCRISPR treatment group show significantly lower lung compliance when compared to Saline group ($p = 0.027$) and no significant difference when compared to the Control group ($p = 1.00$).

Table 39: Kruskal-Wallis Test for full lenti, saline, control

Ranks

	4x LentiComparison	N	Mean Rank
Compliance	Saline Treated	5	12.00
	4x Lenti CRISPR	4	4.75
	Controls	5	5.20
	Total	14	

Test Statisticsa,b

	Compliance
Chi-square	9.026
df	2
Asymp. Sig.	.011

Table 39: Kruskal-Wallis test for lung compliance of 4x lentiCRIPSR, Saline and Control groups demonstrated statistically significant difference between the groups (p = 0.011).

Table 40: Mann-Whitney Test

Ranks

	Group	N	Mean Rank	Sum of Ranks
Compliance	Saline Treated	5	3.20	16.00
	4x Lenti CRISPR	4	7.25	29.00
	Total	9		

Test Statisticsb

	Compliance
Mann-Whitney U	1.000
Wilcoxon W	16.000
Z	-2.205
Asymp. Sig. (2-tailed)	.027
Exact Sig. [2*(1-tailed Sig.)]	.032

Table 40: Mann-Whitney test for lung compliance of 4x lentiCRISPR and Saline groups demonstrated a statistically significant difference between the groups (p = 0.027).

Table 41: Mann-Whitney Test

Ranks

	Group	N	Mean Rank	Sum of Ranks
Compliance	4x Lenti CRISPR	4	5.00	20.00
	Controls	5	5.00	25.00
	Total	9		

Test Statisticsb

	Compliance
Mann-Whitney U	10.000
Wilcoxon W	25.000
Z	.000
Asymp. Sig. (2-tailed)	1.000
Exact Sig. [2*(1-tailed Sig.)]	1.000

Table 41: Mann-Whitney test for lung compliance of 4x lentiCRISPR and Control groups demonstrated no statistically significant difference between the groups (p = 1.00).

5.0 References

1. Arai, S., Arora, M., Wang, T., Spellman, S. R., He, W., Couriel, D. R., & Flowers, M. E. (2015). Increasing incidence of chronic graft-versus-host disease in allogeneic transplantation: a report from the Center for International Blood and Marrow Transplant Research. *Biology of Blood and Marrow Transplantation*, *21*(2), 266-274.
2. Gooptu, Mahasweta, and John Koreth. "Better acute graft-versus-host disease outcomes for allogeneic transplant recipients in the modern era: a tacrolimus effect?." (2017): 806-808.
3. Gyurkocza, B., Rezvani, A., & Storb, R. F. (2010). Allogeneic hematopoietic cell transplantation: the state of the art. *Expert review of hematology*, *3*(3), 285-299.
4. Palmer, Jeanne, et al. "Pulmonary symptoms measured by the national institutes of health lung score predict overall survival, nonrelapse mortality, and patient-reported outcomes in chronic graft-versus-host disease." *Biology of Blood and Marrow Transplantation* 20.3 (2014): 337-344.
5. Ghimire, Sakhila, et al. "Pathophysiology of GvHD and other HSCT-related major complications." *Frontiers in immunology* 8 (2017): 79.
6. Lee, Stephanie J. "New approaches for preventing and treating chronic graft-versus-host disease." *Blood* 105.11 (2005): 4200-4206.
7. Martin, P. J., Storer, B. E., Rowley, S. D., Flowers, M. E., Lee, S. J., Carpenter, P. A., ... & Fay, J. W. (2009). Evaluation of mycophenolate mofetil for initial treatment of chronic graft-versus-host disease. *Blood*, *113*(21), 5074-5082.
8. Nguyen, Hung, et al. "Targeting Host Complement C3a/C5a Receptors to Control of Acute Graft-Versus-Host Disease in Mice." (2015): 3076-3076.
9. Kwan, W. H., Hashimoto, D., Paz-Artal, E., Ostrow, K., Greter, M., Raedler, H. & Heeger, P. S. (2012). Antigen-presenting cell–derived complement modulates graft-versus-host disease. *The Journal of clinical investigation*, *122*(6), 2234.
10. Billingham, R. E., & Silvers, W. K. (1973). Transplantation and cutaneous genetics. *Journal of Investigative Dermatology*, *60*(6), 509-515.
11. Lee, S. J., Klein, J., Haagenson, M., Baxter-Lowe, L. A., Confer, D. L., Eapen, M., & Noreen, H. (2007). High-resolution donor-recipient HLA matching contributes to the success of unrelated donor marrow transplantation. *Blood*, *110*(13), 4576-4583.
12. Svegliati, Silvia, et al. "Stimulatory autoantibodies to PDGF receptor in patients with extensive chronic graft-versus-host disease." *Blood* 110.1 (2007): 237-241.
13. Sarantopoulos, S., Stevenson, K. E., Kim, H. T., Bhuiya, N. S., Cutler, C. S., Soiffer, R. J., ... & Ritz, J. (2007). High levels of B-cell activating factor in patients with active chronic graft-versus-host disease. *Clinical Cancer Research*, *13*(20), 6107-6114.
14. Min, C. K. (2011). The pathophysiology of chronic graft-versus-host disease: the unveiling of an enigma. *The Korean journal of hematology*, *46*(2), 80-87.
15. Kishimoto, H., & Sprent, J. (2000). The thymus and central tolerance. *Clinical Immunology*, *95*(1), S3-S7.
16. Surh, C. D., & Sprent, J. (1994). T-cell apoptosis detected in situ during positive and negative selection in the thymus. *Nature*, *372*(6501), 100.
17. Dutt, S., Tseng, D., Ermann, J., George, T. I., Liu, Y. P., Davis, C. R., ... & Strober, S. (2007). Naive and memory T cells induce different types of graft-versus-host disease. *The Journal of Immunology*, *179*(10), 6547-6554.

18. Zhang, C., Todorov, I., Zhang, Z., Liu, Y., Kandeel, F., Forman, S., ... & Zeng, D. (2006). Donor CD4+ T and B cells in transplants induce chronic graft-versus-host disease with autoimmune manifestations. *Blood*, *107*(7), 2993-3001.
19. Zorn, E., Kim, H. T., Lee, S. J., Floyd, B. H., Litsa, D., Arumugarajah, S., ... & Ritz, J. (2005). Reduced frequency of FOXP3+ CD4+ CD25+ regulatory T cells in patients with chronic graft-versus-host disease. *Blood*, *106*(8), 2903-2911.
20. Clark, F. J., Gregg, R., Piper, K., Dunnion, D., Freeman, L., Griffiths, M., ... & Chakraverty, R. (2004). Chronic graft-versus-host disease is associated with increased numbers of peripheral blood CD4+ CD25 high regulatory T cells. *Blood*, *103*(6), 2410-2416.
21. Sharma, M. D., Baban, B., Chandler, P., Hou, D. Y., Singh, N., Yagita, H., ... & Munn, D. H. (2007). Plasmacytoid dendritic cells from mouse tumor-draining lymph nodes directly activate mature Tregs via indoleamine 2, 3-dioxygenase. *The Journal of clinical investigation*, *117*(9), 2570.
22. Giorgini, A., & Noble, A. (2007). Blockade of chronic graft-versus-host disease by alloantigen-induced CD4+ CD25+ Foxp3+ regulatory T cells in nonlymphopenic hosts. *Journal of leukocyte biology*, *82*(5), 1053-1061.
23. Ratanatharathorn, V., Carson, E., Reynolds, C., Ayash, L. J., Levine, J., Yanik, G., ... & Uberti, J. P. (2000). Anti-CD20 chimeric monoclonal antibody treatment of refractory immune-mediated thrombocytopenia in a patient with chronic graft-versus-host disease. *Annals of internal medicine*, *133*(4), 275-279.
24. Patriarca, F., Skert, C., Sperotto, A., Zaja, F., Falleti, E., Mestroni, R. & Cerno, M. (2006). The development of autoantibodies after allogeneic stem cell transplantation is related with chronic graft-vs-host disease and immune recovery. *Experimental hematology*, *34*(3), 389-396.
25. Svegliati, S., Olivieri, A., Campelli, N., Luchetti, M., Poloni, A., Trappolini, S. & Gabrielli, A. (2007). Stimulatory autoantibodies to PDGF receptor in patients with extensive chronic graft-versus-host disease. *Blood*, *110*(1), 237-241.
26. Cutler, C., Miklos, D., Kim, H. T., Treister, N., Woo, S. B., Bienfang, D., ... & Mac donell, R. (2006). Rituximab for steroid-refractory chronic graft-versus-host disease. *Blood*, *108*(2), 756-762.
27. Shulman, H. M., Kleiner, D., Lee, S. J., Morton, T., Pavletic, S. Z., Farmer, E., ... & McDonald, G. (2006). Histopathologic diagnosis of chronic graft-versus-host disease: National Institutes of Health consensus development project on criteria for clinical trials in chronic graft-versus-host disease: II. Pathology working group report. *Biology of Blood and Marrow Transplantation*, *12*(1), 31-47.
28. Nikolic, B., Lee, S., Bronson, R. T., Grusby, M. J., & Sykes, M. (2000). Th1 and Th2 mediate acute graft-versus-host disease, each with distinct end-organ targets. *Journal of Clinical Investigation*, *105*(9), 1289.
29. Hillebrandt, S., Wasmuth, H. E., Weiskirchen, R., Hellerbrand, C., Keppeler, H., Werth, A., & Köhl, J. (2005). Complement factor 5 is a quantitative trait gene that modifies liver fibrogenesis in mice and humans. *Nature genetics*, *37*(8), 835-843.
30. Tsoi, M. S., Storb, R., Jones, E., Weiden, P. L., Shulman, H., Witherspoon, R., & Thomas, E. D. (1978). Deposition of IgM and complement at the dermoepidermal junction in acute and chronic cutaneous graft-vs-host disease in man. *The Journal of Immunology*, *120*(5), 1485-1492.

31. De Wit, Dominique, et al. "Preferential activation of Th2 cells in chronic graft-versus-host reaction." *The Journal of Immunology* 150.2 (1993): 361-366.
32. Yoon, H. K., Lim, J. Y., Kim, T. J., Cho, C. S., & Min, C. K. (2010). Effects of pravastatin on murine chronic graft-versus-host disease. *Transplantation*, *90*(8), 853-860.
33. Nesargikar, P., Spiller, B., & Chavez, R. (2012). The complement system: history, pathways, cascade and inhibitors. *European Journal of Microbiology and Immunology*, *2*(2), 103-111.
34. Barrington, R., Zhang, M., Fischer, M., & Carroll, M. C. (2001). The role of complement in inflammation and adaptive immunity. *Immunological reviews*, *180*(1), 5-15.
35. Morgan, B. P. (1999). Regulation of the complement membrane attack pathway. *Critical Reviews™ in Immunology*, *19*(3).
36. Takahashi, Minoru, et al. "Mannose-binding lectin (MBL)-associated serine protease (MASP)-1 contributes to activation of the lectin complement pathway." *The Journal of Immunology* 180.9 (2008): 6132-6138.
37. Arumugam, T. V., Shiels, I. A., Woodruff, T. M., Granger, D. N., & Taylor, S. M. (2004). The role of the complement system in ischemia-reperfusion injury. *shock*, *21*(5), 401-409.
38. Diepenhorst, G. M., van Gulik, T. M., & Hack, C. E. (2009). Complement-mediated ischemia-reperfusion injury: lessons learned from animal and clinical studies. *Annals of surgery*, *249*(6), 889-899.
39. Mevorach, D., Mascarenhas, J. O., Gershov, D., & Elkon, K. B. (1998). Complement-dependent clearance of apoptotic cells by human macrophages. *Journal of Experimental Medicine*, *188*(12), 2313-2320.
40. van Kooten, C., Fiore, N., Trouw, L. A., Csomor, E., Xu, W., Castellano, G., & Gelderman, K. A. (2008). Complement production and regulation by dendritic cells: molecular switches between tolerance and immunity. *Molecular immunology*, *45*(16), 4064-4072.
41. Lubbers, R., van Essen, M. F., van Kooten, C., & Trouw, L. A. (2017). Production of complement components by cells of the immune system. *Clinical & Experimental Immunology*.
42. Pouzolles, Marie, et al. "Hematopoietic stem cell lineage specification." *Current opinion in hematology* 23.4 (2016): 311-317.
43. Höfer, Thomas, and Hans-Reimer Rodewald. "Differentiation-based model of hematopoietic stem cell functions and lineage pathways." *Blood* 132.11 (2018): 1106-1113.
44. Liu, Kang, and Michel C. Nussenzweig. "Origin and development of dendritic cells." *Immunological reviews* 234.1 (2010): 45-54.
45. Kamath, Arun T., et al. "The development, maturation, and turnover rate of mouse spleen dendritic cell populations." *The Journal of Immunology* 165.12 (2000): 6762-6770.
46. Hashimoto, Daigo, et al. "Tissue-resident macrophages self-maintain locally throughout adult life with minimal contribution from circulating monocytes." *Immunity* 38.4 (2013): 792-804.
47. Flowers, M. E., Inamoto, Y., Carpenter, P. A., Lee, S. J., Kiem, H. P., Petersdorf, E. W., and Warren, E. H. (2011). Comparative analysis of risk factors for acute graft-versus-host disease and for chronic graft-versus-host disease according to National Institutes of Health consensus criteria. *Blood*, *117*(11), 3214-3219.

48. Lee, S. J., & Flowers, M. E. (2008). Recognizing and managing chronic graft-versus-host disease. *ASH Education Program Book*, *2008*(1), 134-141.
49. Wolff, D., Gerbitz, A., Ayuk, F., Kiani, A., Hildebrandt, G. C., Vogelsang, G. B., & Holler, E. (2010). Consensus conference on clinical practice in chronic graft-versus-host disease (GVHD): first-line and topical treatment of chronic GVHD. *Biology of Blood and Marrow Transplantation*, *16*(12), 1611-1628.
50. Flowers, M. E., & Martin, P. J. (2014). How we treat chronic graft-versus-host disease. *Blood*, blood-2014.
51. Jabs, K., Sullivan, E. K., Avner, E. D., & Harmon, W. E. (1996). Alternate-day steroid dosing improves growth without adversely affecting graft survival or long-term graft function: A Report of the North American Pediatric Renal Transplant Cooperative Study1, 2, 3. *Transplantation*, *61*(1), 31-36.
52. Martin, P. J., Storer, B. E., Rowley, S. D., Flowers, M. E., Lee, S. J., Carpenter, P. A., ... & Fay, J. W. (2009). Evaluation of mycophenolate mofetil for initial treatment of chronic graft-versus-host disease. *Blood*, *113*(21), 5074-5082.
53. Lee, S. J., Klein, J. P., Barrett, A. J., Ringden, O., Antin, J. H., Cahn, J. Y., ... & Ilhan, O. (2002). Severity of chronic graft-versus-host disease: association with treatment-related mortality and relapse. *Blood*, *100*(2), 406-414.
54. Ran, F. Ann, et al. "Genome engineering using the CRISPR-Cas9 system." *Nature protocols* 8.11 (2013): 2281.
55. Garneau, J. E., Dupuis, M. E., Villion, M., Romero, D. A., Barrangou, R., Boyaval, P., & Moineau, S. (2010). The CRISPR/Cas bacterial immune system cleaves bacteriophage and plasmid DNA. *Nature*, *468*(7320), 67-71.
56. Jinek, Martin, et al. "A programmable dual-RNA–guided DNA endonuclease in adaptive bacterial immunity." *Science* 337.6096 (2012): 816-821.
57. Cong, Le, et al. "Multiplex genome engineering using CRISPR/Cas systems." *Science* 339.6121 (2013): 819-823.
58. Mali, Prashant, et al. "RNA-guided human genome engineering via Cas9." *Science* 339.6121 (2013): 823-826.
59. Saleh-Gohari, N., & Helleday, T. (2004). Conservative homologous recombination preferentially repairs DNA double-strand breaks in the S phase of the cell cycle in human cells. *Nucleic acids research*, *32*(12), 3683-3688.
60. Ran, F. Ann, et al. "Double nicking by RNA-guided CRISPR Cas9 for enhanced genome editing specificity." *Cell* 154.6 (2013): 1380-1389.
61. Reyon, D., Tsai, S. Q., Khayter, C., Foden, J. A., Sander, J. D., & Joung, J. K. (2012). FLASH assembly of TALENs for high-throughput genome editing. *Nature biotechnology*, *30*(5), 460-465.
62. Urnov, F. D., Rebar, E. J., Holmes, M. C., Zhang, H. S., & Gregory, P. D. (2010). Genome editing with engineered zinc finger nucleases. *Nature Reviews Genetics*, *11*(9), 636-646.
63. Chen, F., Pruett-Miller, S. M., Huang, Y., Gjoka, M., Duda, K., Taunton, J., & Davis, G. D. (2011). High-frequency genome editing using ssDNA oligonucleotides with zinc-finger nucleases. *Nature methods*, *8*(9), 753-755.
64. Hsu, Patrick D., et al. "DNA targeting specificity of RNA-guided Cas9 nucleases." *Nature biotechnology* 31.9 (2013): 827.

65. O'Keefe, E. P. "Nucleic acid delivery: lentiviral and retroviral vectors." *Labome com* (2013).
66. Wain-Hobson, Simon. "Retrovirus evolution." *Origin and Evolution of Viruses (Second Edition)*. 2008. 259-277.
67. Warnock J, Daigre C, Al Rubeai M. Introduction to viral vectors. Methods Mol Biol. 2011;737:1-25
68. Tiscornia, Gustavo, Oded Singer, and Inder M. Verma. "Production and purification of lentiviral vectors." *Nature protocols* 1.1 (2006): 241.
69. Sakuma, Toshie, Michael A. Barry, and Yasuhiro Ikeda. "Lentiviral vectors: basic to translational." *Biochemical Journal* 443.3 (2012): 603-618.
70. Cockrell, Adam S., and Tal Kafri. "Gene delivery by lentivirus vectors." *Molecular biotechnology* 36.3 (2007): 184-204.
71. Naldini, Luigi, et al. "In vivo gene delivery and stable transduction of nondividing cells by a lentiviral vector." *Science* 272.5259 (1996): 263-267.
72. Sanjana, Neville E., Ophir Shalem, and Feng Zhang. "Improved vectors and genome-wide libraries for CRISPR screening." *Nature methods* 11.8 (2014): 783.
73. Doench, John G., et al. "Optimized sgRNA design to maximize activity and minimize off-target effects of CRISPR-Cas9." *Nature biotechnology* 34.2 (2016): 184.
74. Holmgaard, Andreas, et al. "In vivo knockout of the Vegfa gene by lentiviral delivery of CRISPR/Cas9 in mouse retinal pigment epithelium cells." *Molecular Therapy-Nucleic Acids* 9 (2017): 89-99.
75. Wang, Xuefeng, et al. "Intraosseous delivery of lentiviral vectors targeting factor VIII expression in platelets corrects murine hemophilia A." *Molecular Therapy* 23.4 (2015): 617-626.
76. Imani, J., Ayaub, E., Wattie, J., Wang, I., Inman, M., Kolb, M., Margetts, P., Larche, M. Donor-derived C5 is required for induction of murine Pulmonary GVHD following hematopoietic stem cell transplant. Submitted to: Blood (2018, August)
77. Miklos, Sandra, et al. "Pulmonary function changes in experimental graft-versus-host disease of the lung." *Biology of Blood and Marrow Transplantation* 14.9 (2008): 1004-1016.
78. Plantier, Laurent, et al. "Physiology of the lung in idiopathic pulmonary fibrosis." *European Respiratory Review* 27.147 (2018): 170062.
79. Hart, Nicholas, et al. "Changes in pulmonary mechanics with increasing disease severity in children and young adults with cystic fibrosis." *American journal of respiratory and critical care medicine* 166.1 (2002): 61-66.
80. Papandrinopoulou, D., V. Tzouda, and G. Tsoukalas. "Lung compliance and chronic obstructive pulmonary disease." *Pulmonary medicine* 2012 (2012).
81. Ferrara, Giovanni B., et al. "Bone marrow transplantation from unrelated donors: the impact of mismatches with substitutions at position 116 of the human leukocyte antigen class I heavy chain." *Blood* 98.10 (2001): 3150-3155.
82. Körbling, Martin, and Paolo Anderlini. "Peripheral blood stem cell versus bone marrow allotransplantation: does the source of hematopoietic stem cells matter?." *Blood* 98.10 (2001): 2900-2908.
83. Sonntag, J., et al. "Complement system in healthy term newborns: reference values in umbilical cord blood." *Pediatric and Developmental Pathology* 1.2 (1998): 131-135.